Plant Physiology®

NAC transcription factor TgNAP promotes tulip petal senescence

Lin Meng [iD] ,[1,2] Haipo Yang [iD] ,[1,2] Lin Xiang,[1] Yanping Wang [iD] [1,2,*] and Zhulong Chan [iD] [1,*,†]

1 Key Laboratory of Horticultural Plant Biology, Ministry of Education, College of Horticulture and Forestry Sciences, Huazhong Agricultural University, Wuhan 430070, PR China
2 National R&D Centre for Citrus Preservation, Huazhong Agricultural University, Wuhan 430070, PR China

*Author for correspondence: zlchan@mail.hzau.edu.cn (Y.W.), ypwang@mail.hzau.edu.cn (Z.C.)
†Senior author
L.M. conducted the experiments. H.Y. collected the data. Y.W., Z.C., and L.M. designed the experiments and wrote the paper. Z.C., Y.W., and L.X. revised the manuscript.
The author responsible for distribution of materials integral to the findings presented in this article in accordance with the policy described in the Instructions for Authors (https://academic.oup.com/plphys/pages/general-instructions) is: Zhulong Chan (zlchan@mail.hzau.edu.cn).

Abstract

Petal senescence is a crucial determinant for ornamental quality and economic value of floral crops. Salicylic acid (SA) and reactive oxygen species (ROS) are two prominent factors involved in plant senescence regulation. In this study, tulip *TgNAP* (NAC-like, activated by APETALA3/PISTILLATA) was characterized as positively regulating tulip petal senescence through dually regulating SA biosynthesis and ROS detoxification pathways. *TgNAP* was upregulated in senescing petals of tulip while exogenous SA and H_2O_2 treatments substantially promoted petal senescence in tulip. Silencing of *TgNAP* by VIGS assay delayed SA and H_2O_2-induced petal senescence in tulip, whereas overexpression of *TgNAP* promoted the senescence process in Arabidopsis (*Arabidopsis thaliana*) plants. Additionally, inhibition of SA biosynthesis prolonged the lifespan of *TgNAP*-silenced petal discs. Further evidence indicated that TgNAP activates the transcriptions of two key SA biosynthetic genes *ISOCHORISMATE SYNTHASE 1* (*TgICS1*) and *PHENYLALANINE AMMONIA-LYASE 1* (*TgPAL1*) through directly binding to their promoter regions. Meanwhile, TgNAP repressed ROS scavenging by directly inhibiting *PEROXIDASE 12* (*POD12*) and *POD17* expression. Taken together, these results indicate that TgNAP enhances SA biosynthesis and ROS accumulation to positively regulate petal senescence in tulip.

Introduction

Plant senescence is the last stage during the whole developmental process, eventually resulting in death of cells, tissues, and organisms (Gan and Amasino, 1997; Zhang et al., 2021). Senescence generally occur in different organs, such as leaves, stems, roots, and petals (Schippers et al., 2015; Woo et al., 2019). Petal senescence is a complicated process and closely related to economic value of ornamental plants (Tripathi and Tuteja, 2007; Rogers, 2013; Ma et al., 2018). Plant senescence is regulated not only by internal factors such as natural aging, reproduction, reactive oxygen species (ROS), hormones, and sugar, but also by external factors including dehydration, temperature, light, ionic accumulation, nutrition limitation, and pathogen attack or wounding (Gan and Amasino, 1997; Woo et al., 2013; Zhao et al., 2016; Mhamdi and Van Breusegem, 2018). Among plant hormones, cytokinin (CTK) and gibberellins (GAs) are considered to retard senescence, while abscisic acid (ABA), ethylene (ETH), and salicylic acid (SA) are commonly regarded as aging-promoting hormones (Gan and Amasino, 1997; Morris et al., 2000; He et al., 2002; Zhao et al., 2016;

Lee et al., 2021). As crucial plant hormones, ethylene and ABA have been well studied to participate in leaf senescence. Moreover, further studies have revealed that NAC TF family plays a vital role in ethylene- and ABA-induced leaf senescence. In maize (*Zea mays*), ZmNAC126 acts as a positive regulator in ethylene-induced leaf senescence functioning downstream of *ZmEIN3* (*ETHYLENE-INSENSITIVE3*; Yang et al., 2020). ORESARA1 (ORE1), a NAC transcription factor in Arabidopsis (*Arabidopsis thaliana*), is also able to promote leaf senescence in ethylene signaling pathway by activating the expression of *1-AMINOCYCLOPROPANE-1-CARBOXYLIC SYNTHASE2* (*ACS2*; Qiu et al., 2015). Tomato (*Solanum lycopersicum*) SlNAP2 directly upregulates expression of *SlSAG113* (*SENESCENCE-ASSOCIATED GENE113*) and ABA biosynthesis-related gene *SlNCED1* (*9-cis-EPOXYCAROTENOID DIOXYGENASE 1*) to promote leaf senescence and establish ABA homeostasis (Ma et al., 2018). *OsNAC2* increases ABA levels via regulating expression of ABA biosynthetic genes (Mao et al., 2017).

A growing body of evidence indicates that SA plays important roles in natural senescence process (Rivas-San Vicente and Plasencia, 2011; Zhang et al., 2013). SA level was 4-fold higher in senescing leaves when compared to young leaves (Morris et al., 2000), and SA accumulation further led to premature senescence in leaves (Vogelmann et al., 2012; Li et al., 2016). SA induced the expression of a couple of senescence-associated genes (*SAGs*; Wang et al., 2021a). Meanwhile, about 20% of senescence-enhanced genes exhibit substantially decreased expression in SA-deficient *NahG* transgenic Arabidopsis (Morris et al., 2000). Arabidopsis mutants including *pad4* and *npr1*, which are defective in SA signaling pathway, showed delayed senescence phenotype and a great reduction of *SAGs* expression (Morris et al., 2000; Woo et al., 2019). Moreover, transcriptome analysis shows an intriguing observation that SA treatment has similar genomic change patterns with age-mediated leaf senescence (Pyung et al., 2007), further suggesting the positive role of SA in senescence progress.

ROS not only acts as toxic by-product, but also as signaling molecules to regulate development, growth, and defense response of plants (Miller et al., 2010; Huang et al., 2016). The excessive ROS production might damage macromolecules stabilization resulting in senescence initiation and cell death (Miller et al., 2010). H_2O_2 contents increase in different senescing plants, such as senescing peach (*Prunus persica*) fruit (Wu et al., 2016), ripening tomato (Jimenez et al., 2002), and Arabidopsis aged yellow leaf (Niu et al., 2020; Wang et al., 2020a). The cross-talk between oxidative burst and SA has been extensively reported. Recent studies have revealed that SA and ROS pathways are incorporated to modulate senescence process in plants (Guo et al., 2017). SA can induce the ROS accumulation (Rao et al., 1997; Wang et al., 2021b) and H_2O_2 also elicits the generation of SA (León et al., 1995). Altering SA biosynthesis resulted in a modulation of the catalase (*CAT*) expression, indicating that ROS function as upstream regulator of SA pathway (Han

et al., 2013). Additionally, SA conversely regulates ROS accumulation through inhibiting antioxidant enzymes activities and reducing glutathione biosynthesis (Chen et al., 1993; Vlot et al., 2009). Therefore, the interactions between SA and ROS are complicated.

Transcriptional analysis has proved that a number of TFs are involved in senescence process in various plant species, including WRKYs, ERFs, MYBs, bHLH, homeobox, and NACs (NAM/ATAF/CUC), which further regulate expressions of downstream senescence associate genes (Lü et al., 2014; Song et al., 2014; Chen et al., 2017; Guo et al., 2017; Niu et al., 2020; Wang et al., 2020a; Yu et al., 2022). In Arabidopsis, 57.5% (65/113) of NAC genes exhibited expression changes during leaf senescence. Genetic study revealed that ANAC002/ATAF1, ANAC016, ANAC017/NTL7, ANAC019, ANAC029/AtNAP, ANAC059/ORS1, ANAC081/ATAF2, ANAC092/ORE1, and ANAC096 function as positive regulators of leaf senescence (Guo and Gan, 2006; Balazadeh et al. 2011; Wu et al., 2012; Kim et al., 2013; Nagahage et al., 2020). Balazadeh et al. (2010) identified 170 downstream genes induced by ANAC092/ORE1 and found that 46% of them are known to be involved in senescence pathway. *ANAC059/ORS1* was induced by H_2O_2 treatment to trigger expression of senescence-associated gene regulatory networks which accelerated plant senescence (Balazadeh, et al. 2011). Other NACs, including ANAC042/JUB1, ANAC075/NAC075, and ANAC083/VNI2 in Arabidopsis, and LpNAL in perennial ryegrass (*Lolium perenne* L.) were reported to be negative regulators of leaf senescence (Yang et al., 2011; Wu et al., 2012; Kan et al., 2021; Yu et al., 2022). NAC transcription factor *VNI2* was induced by ABA and delayed leaf aging through binding to the promoters of COR and RD genes (Yang et al., 2011). NAC genes *NTL9*, *ATAF2*, and *CaNAC1* were substantially induced by SA and involved in biotic stress and leaf senescence (Delessert et al., 2005; Oh et al., 2005; Zheng et al., 2015; Nagahage et al., 2020). Recently, ANAC017, ANAC082, and ANAC090 were reported to negatively regulate leaf senescence by suppressing SA and ROS pathways (Kim et al., 2018). It is suggested that NAC TF may play a crucial role in SA signaling pathway. NAC075 activates *CAT2* to reduce ROS accumulation and negatively regulates leaf senescence (Kan et al., 2021). H_2O_2 treatment was reported to induce the expression of several senescence-associated NACs, such as ANAC029/AtNAP, ANAC002/ATAF1, ANAC042/JUB1, and ANAC059/ORS1 (Guo and Gan, 2006; Balazadeh, 2011; Wu et al., 2012). However, the detailed regulatory networks among NAC, SA, and ROS remain largely unknown.

ANAC090 of Arabidopsis negatively regulates leaf senescence by suppressing SA and ROS responses (Kim et al., 2018). In this study, however, we found that *TgNAP* promotes petal senescence in tulip (*Tulipa gesneriana*) through activation of SA biosynthesis and ROS detoxification pathways. *TgNAP* was identified as one of the substantially upregulated NACs in senescing tulip petals. The leaf senescence was promoted in *TgNAP* overexpressed transgenic plants,

while *TgNAP* silencing expression delayed petal disc aging. TgNAP modulated SA biosynthesis and H_2O_2 accumulation by directly activating *TgICS1* and *TgPAL1* transcription, and inhibiting expressions of ROS scavenging genes *TgPOD12* and *TgPOD17*. We report here that TgNAP functions as a positive regulator during tulip petal senescence partially in SA- and H_2O_2-dependent manners.

Results

Transcriptomic analysis during petal senescence in tulip

We previously investigated physiological and metabolite changes during tulip petal senescence (Wang et al., 2020b). RNA sequencing was performed to further dissect transcriptomic changes of tulip petal at five developmental stages. The results showed that 1967/1188, 3477/2644, 6252/5581 and 5871/3955 unigenes exhibited significant up-/downregulation from S2 to S5 stages when compared to S1 stage (Figure 1, A and B; Supplemental Table S1). Among them, 810 and 641 unigenes were commonly upregulated and downregulated at all developmental stages, respectively. Meanwhile, 1,987 and 1,173 unigenes were co-upregulated and co-downregulated only at petal senescence stages (S4_vs_S1 and S5_vs_S1; Figure 1, A and B; Supplemental Table S2). Protein interaction network analysis revealed that NAC transcription factor together with ROS, SA, ABA, and ET pathways-related genes functioned as the core nodes (Supplemental Figure S1a). We further obtained the expression patterns of *NAC* family genes in tulip. Totally 52 annotated *NAC* unigenes were identified. Unigenes F01.PB833 and F01.PB17010 were annotated as NAC029 and displayed relatively low expression during early blooming stages (S1–S3 stages) but had substantially increase in tulip petal at senescence stage (S4 and S5 stages; Figure 1C; Supplemental Table S3).

As SA and ROS pathways are closely related with differential NACs during petal senescence in tulip, the expression of two SA biosynthesis-related genes and ROS scavenging genes were examined, respectively. *TgPAL1* showed an obvious elevation from S2 to S4, peaking at S3 (Figure 1D; Supplemental Figure S1b). RT-qPCR results showed that *TgICS1* exhibited steady upregulation during petal senescence (Supplemental Figure S1c). Heatmap and RT-qPCR results showed that *TgPOD12* and *TgPOD17* exhibited a marked decrease during senescence stage (Figure 1D; Supplemental Figure S1, d and e).

TgNAP is a petal senescence-related gene induced by SA

The open reading frame (ORF) of F01.PB833 is 765 bp, encoding a protein of 255 amino acids. Phylogenetic tree analysis indicated that F01.PB833 obtained the most similarity to AtNAC29 (AtNAP; Supplemental Figure S2a), which was thereby named as *TgNAP*. Protein domain analysis showed that TgNAP contains a conserved N-terminal region, including A–E five subdomains (Supplemental Figure S2b).

TgNAP was localized to the nucleus in *Nicotiana tabacum* epidermal cells (Figure 2A). Truncated assay indicated that C terminus is essential for TgNAP transcriptional activation in yeast (Figure 2, B and C). Transcription level of *TgNAP* was confirmed by RT-qPCR. The results showed relatively lower expression at Stages 2 and 3 but significantly higher levels at Stages 4 and 5 (Figure 2D). Furthermore, *TgNAP* expression was induced greatly and significantly in tulip petals by exogenous SA treatment (Figure 2E). These results demonstrate that *TgNAP* is a tulip petal senescence-related gene induced by SA.

Silencing of *TgNAP* delays petal senescence and inhibits SA synthesis in tulip

To further explore the potential role of *TgNAP* in petal senescence in tulip, *TgNAP* was silenced using virus-induced gene silencing (VIGS) method. The downregulated level of *TgNAP* was verified by genomic PCR (Supplemental Figure S3a) and RT-qPCR in *TgNAP* silenced petal discs and flowers (Figure 3A; Supplemental Figure S3b). The control petal discs exhibited color fading at Day 3 and completely turned yellow on Day 5 (Figure 3B). Conversely, silencing of *TgNAP* visibly delayed the petal senescence and only showed slight color fading on Day 5 (Figure 3B). In line with the phenotypic differences, significantly higher anthocyanin content and reduced transcript level of *TgSAG6*, which is the marker gene of senescence in tulip (Wang et al., 2020b), were observed in *TgNAP* silenced petal discs when compared to TRV2 control discs (Figure 3, C and D). In addition, SA biosynthesis genes *TgICS1* and *TgPAL1* were significantly repressed in TRV2-*TgNAP* (Figure 3, E and F) which was evidenced by reduced SA content in TRV2-*TgNAP* petal discs when compared to TRV2 control (Figure 3G). The flower longevity of TRV2 control flowers was significantly longer than that of TRV2-*TgNAP* (Supplemental Figure S3, c and d). The above results illustrated that *TgNAP* is involved in senescence process and SA biosynthesis in tulip petals.

Ectopic overexpression of *TgNAP* facilitates SA synthesis and leaf senescence

To confirm the potential role of *TgNAP* in plant senescence, transgenic Arabidopsis lines overexpressing *TgNAP* under the control of the cauliflower mosaic virus (CaMV) 35S promoter, were generated (Supplemental Figure S4, a–c). Under normal growth condition, no morphological differences were observed between the transgenic and wild-type plants during vegetative stage (Supplemental Figure S4a). However, *TgNAP*-OE transgenic lines exhibited a precocious rosette leaf senescence phenotype with more yellow mature leaves than WT plants on the 28th day after planting (Supplemental Figure S4b). Consistently, the chlorophyll content in *TgNAP*-OE rosette leaves was notably lower than that in WT (Supplemental Figure S4f). Additionally, the expressions of two senescence marker genes *AtSAG12* and *AtSAG13* were significantly induced in transgenic plants relative to WT (Supplemental Figure S4, d and e). *TgNAP*-OE
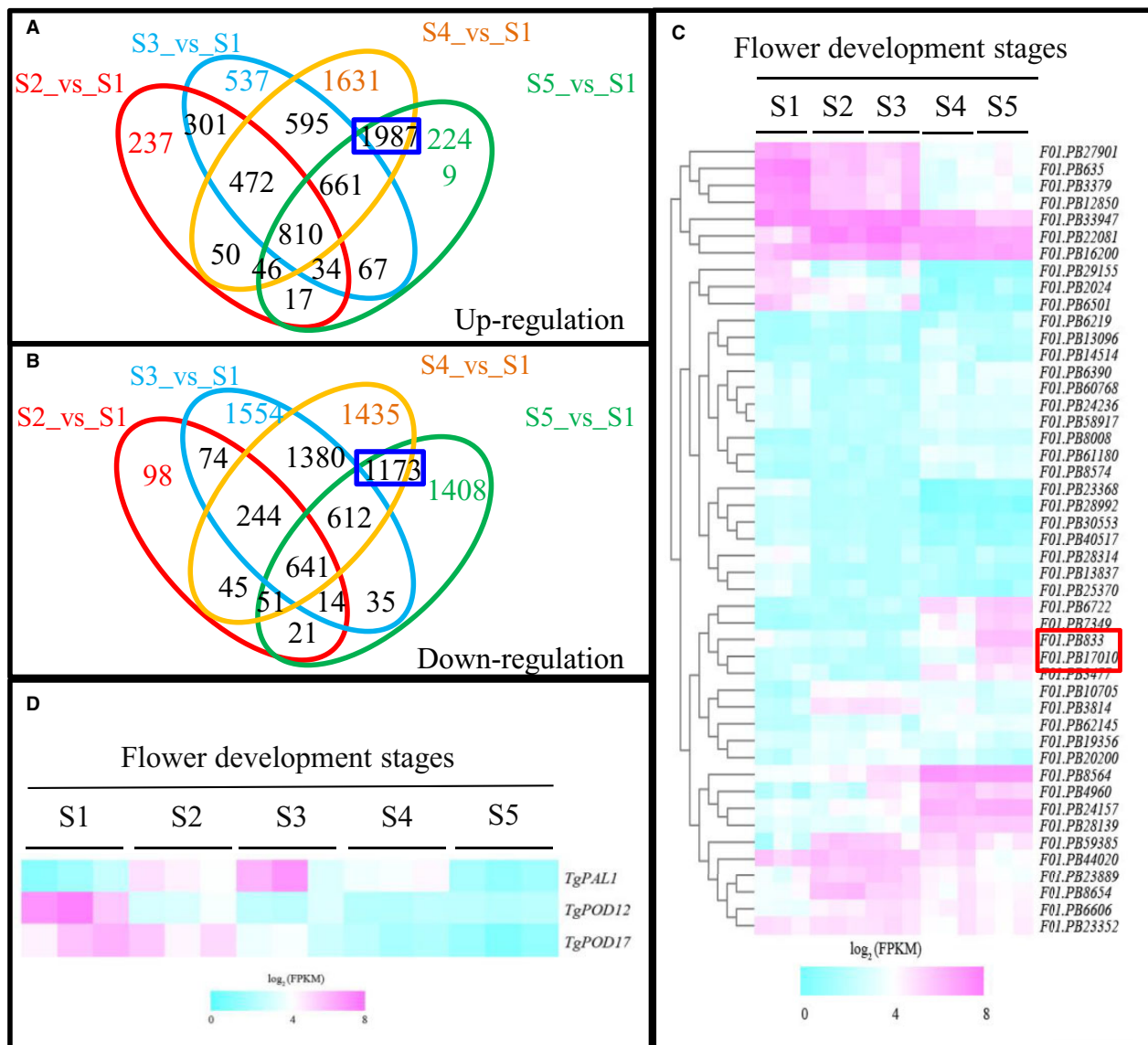
Figure 1 RNA sequencing analysis during petal senescence of *T. gesneriana*. A and B, Overlapping analysis of differentially expressed unigenes. (A) Upregulation, (B) Downregulation. C, Expression profiles of 52 *NAC* genes in *T. gesneriana* during petal senescence. Two unigenes F01.PB17010 and F01.PB833 annotated as NAC029 were highlighted with red box. GFB (the first stage, S1), CFB (the second stage, S2), flowers in FB (the third stage, S3), flowers in ESP (the fourth stage, S4), and flowers in LSP (the fifth stage, S5). D, Expression profiles of *TgPAL1*, *TgPOD12*, and *TgPOD17* in *T. gesneriana* during petal senescence.

transgenic plants also exhibited significantly higher H_2O_2 content when compared to WT (Supplemental Figure S4g).

Since SA level significantly increased in senescence tulip petal and *TgNAP* expression was markedly upregulated after SA treatment (Figure 2E), *TgNAP* could putatively promote petal senescence via SA-associated pathway. To verify the speculation, SA contents were measured in WT and *TgNAP*-OE transgenic Arabidopsis plants. The results revealed that SA level was significantly enhanced in *TgNAP*-OE lines when compared to WT (Supplemental Figure S4h). Moreover, the expressions of SA biosynthesis-related genes *AtSID2*, *AtPAL1*, *AtEPS5*, and *AtEPS1* were significantly higher in *TgNAP*-OE than those in WT (Supplemental Figure S4, i–l). These results indicated that overexpression of *TgNAP* notably

promoted leaf senescence in Arabidopsis via activating SA biosynthesis pathway.

TgNAP promotes senescence in an SA-dependent manner

To explore if SA accumulation is necessary for *TgNAP*-promoted tulip petal senescence, the effect of SA and SA synthesis inhibitor (2-aminoindan-2-phosphonic acid, AIP; Solecka and Kacperska, 2013) on tulip petal and Arabidopsis leaf were further investigated. In the presence of AIP, petal senescence was obviously retarded as evidenced by similar color fading between TRV2-*TgNAP* and TRV2 (Figure 4A). Consistently, AIP treatment delayed anthocyanin
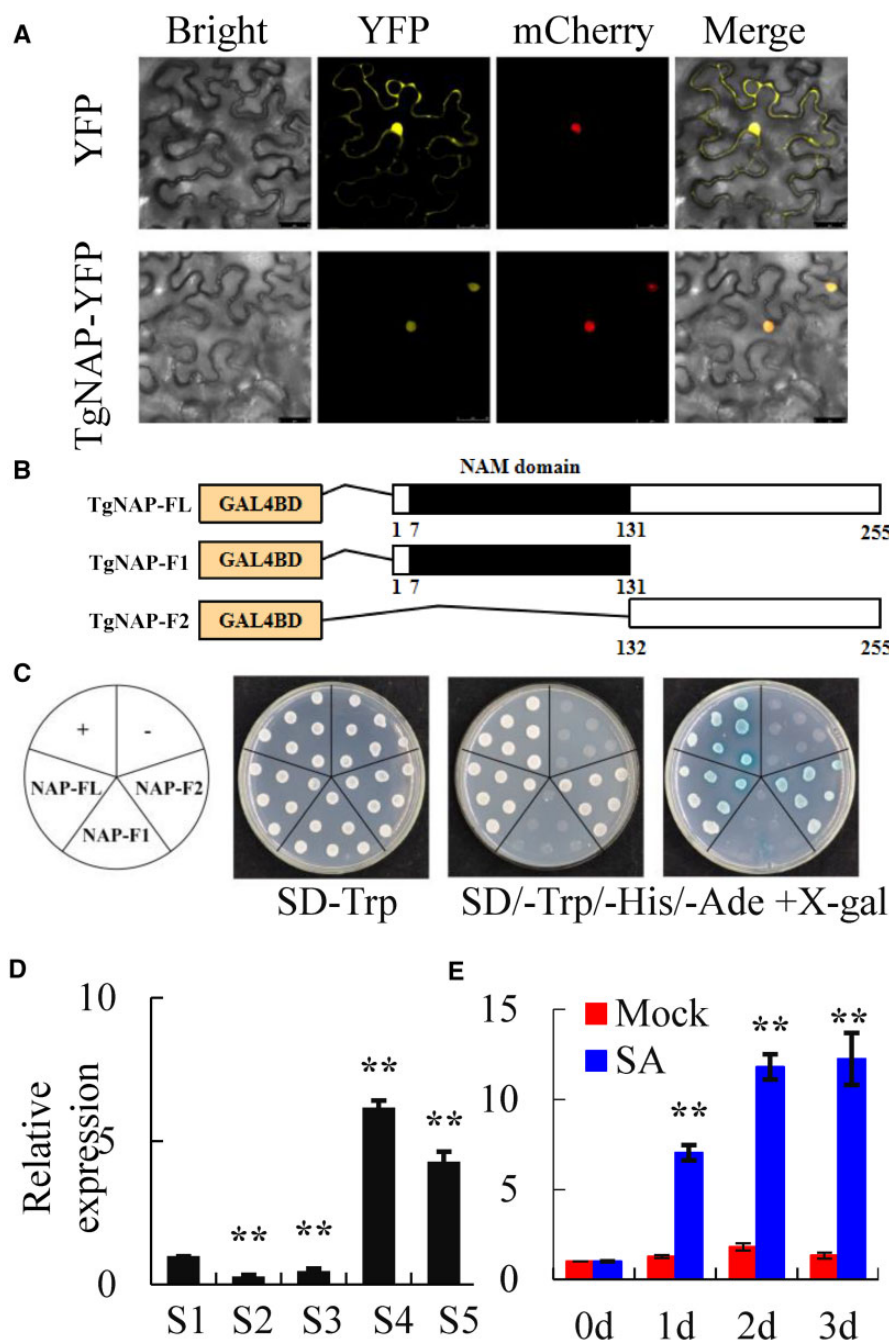
Figure 2 Characterization of *TgNAP* during petal senescence in *T. gesneriana*. A, Subcellular location of TgNAP. The fusion construct TgNAP-YFP or YFP empty vector was co-transformed with *VirD2NLS*-mCherry (a nucleus marker) in *N. benthamiana* leaves. Confocal microscopic images showed bright field, yellow (for YFP), red (for mCherry) fluorescence signals in epidermal cells. Scale bars = 25 μm. B, Schematic diagrams of the full length (FL) and two truncated fragments (F1 and F2) of TgNAP used for constructing vectors. All constructed vectors were introduced in pGBKT7 vector with GAL4 DBD domain. The numbers below the bars indicate the positions of amino acid. C, Transcription activity assay. Growth of yeast cell (AH109 strain) transformed with various constructed vectors on SD/-Trp and SD/-Trp/-His/-Ade with or without X-α-gal selective medium. Transformation of pGBKT7-p53 and pGBKT7 vector was used as a positive and negative control, respectively. D and E, RT-qPCR analysis of *TgNAP* expression levels in *T. gesneriana* during petal senescence (D) or treated with 200 μM SA for 3 d (E). S1–S5 are abbreviations of first stage to fifth stage. The expression levels of the samples at the indicated time point were normalized to a *TgUBQ10-like* gene. Relative gene expression was calculated using the $2^{-\Delta\Delta Ct}$ method. Error bars represent ± SE ($n = 3$). Asterisks indicate significant difference between WT and two transgenic lines based on the LSD values (**$P < 0.01$).

degradation in TRV2 control petal discs as evidenced by similar anthocyanin contents between TRV2 and TRV2-*TgNAP* petal discs in the presence of AIP (Figure 4B). Additionally,

TgSAG6 transcript was significantly reduced in both TRV2 and TRV2-*TgNAP* petal discs after AIP treatment (Figure 4C). TRV2 petal discs obtained significantly higher H$_2$O$_2$
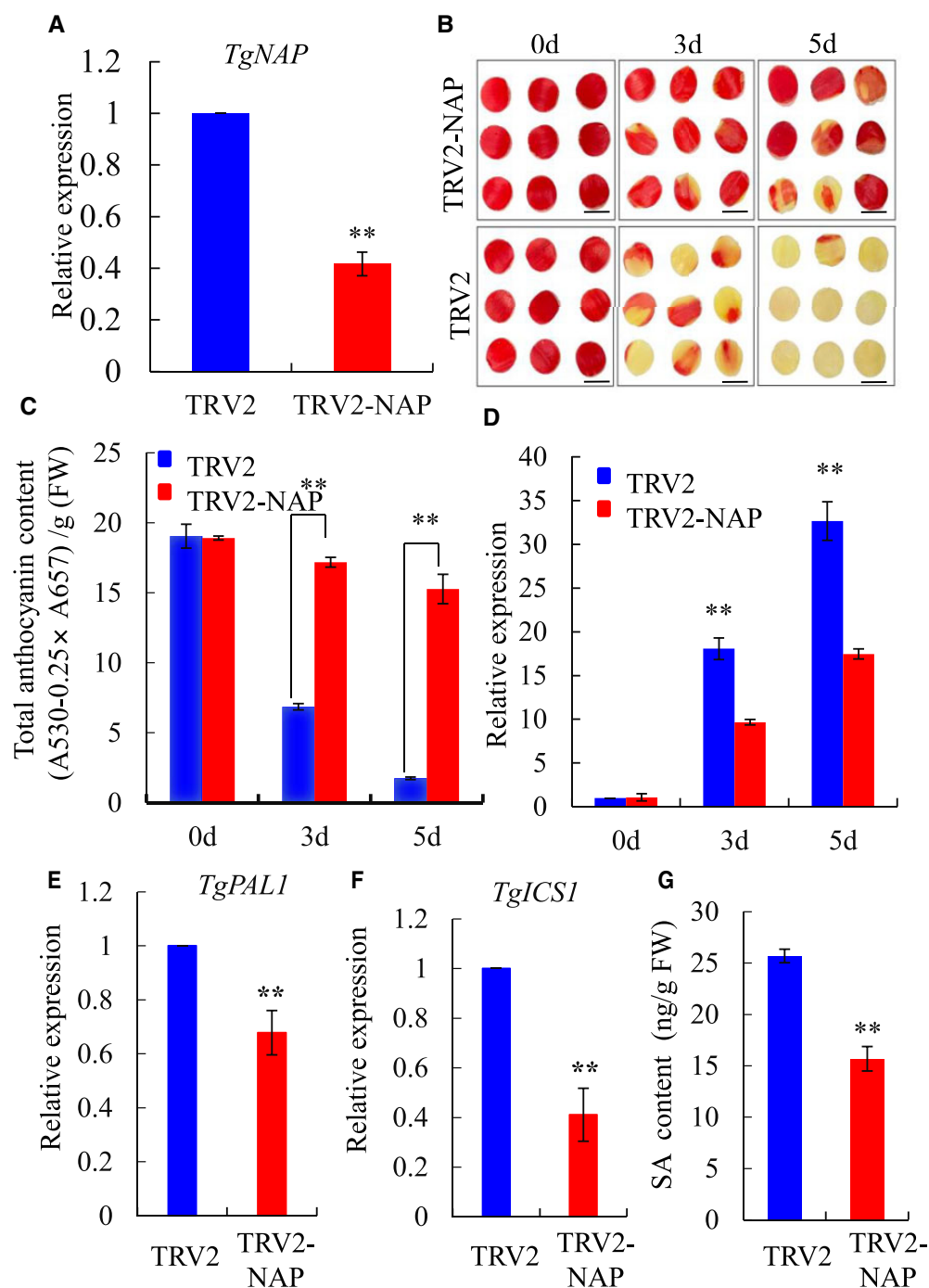
Figure 3 Silencing of *TgNAP* delayed senescence in tulip petal discs. A, Expression levels of *TgNAP* in the TRV2 control and *TgNAP*-silenced petals at Day 3 by RT-qPCR analysis. The expression levels of the samples at the indicated time point were normalized to a *TgUBQ10-like* gene. Relative gene expression was calculated using the $2^{-\Delta\Delta Ct}$ method. B, Phenotypes of tulip petal discs detached from TRV2 control and TRV2-*TgNAP* line under ambient conditions. Scale bar, 1 cm. The samples in each boxed area were photographed at the same time and are part of a single image. C, Total anthocyanin levels of TRV control and *TgNAP*-silenced petals. D, Expression levels of *TgSAG6* of TRV2 control and *TgNAP*-silenced petals. E and F, Expression levels of *TgPAL1* (E) and *TgICS1* (F) of TRV2 control and *TgNAP*-silenced petals at Day 3. The expression levels of the samples at the indicated time point were normalized to a *TgUBQ10-like* gene. Relative gene expression was calculated using the $2^{-\Delta\Delta Ct}$ method. G, SA content in TRV2 control and *TgNAP*-silenced petals at Day 5. Error bars indicate SE (*n* = 3). Asterisks indicate significant difference between the *TgNAP*-silenced petals and the TRV control based on the LSD values (**$P < 0.01$).

accumulation in the absence of AIP than TRV2-*TgNAP*, however, AIP treatment resulted in similar H_2O_2 contents in TRV2-*TgNAP* and TRV2 petal discs (Figure 4, D and E).

Furthermore, the 7–8 rosette leaves from 28-d-old WT and *TgNAP*-OE transgenic Arabidopsis were detached and treated with AIP and SA, respectively. After SA treatment for 3 d,
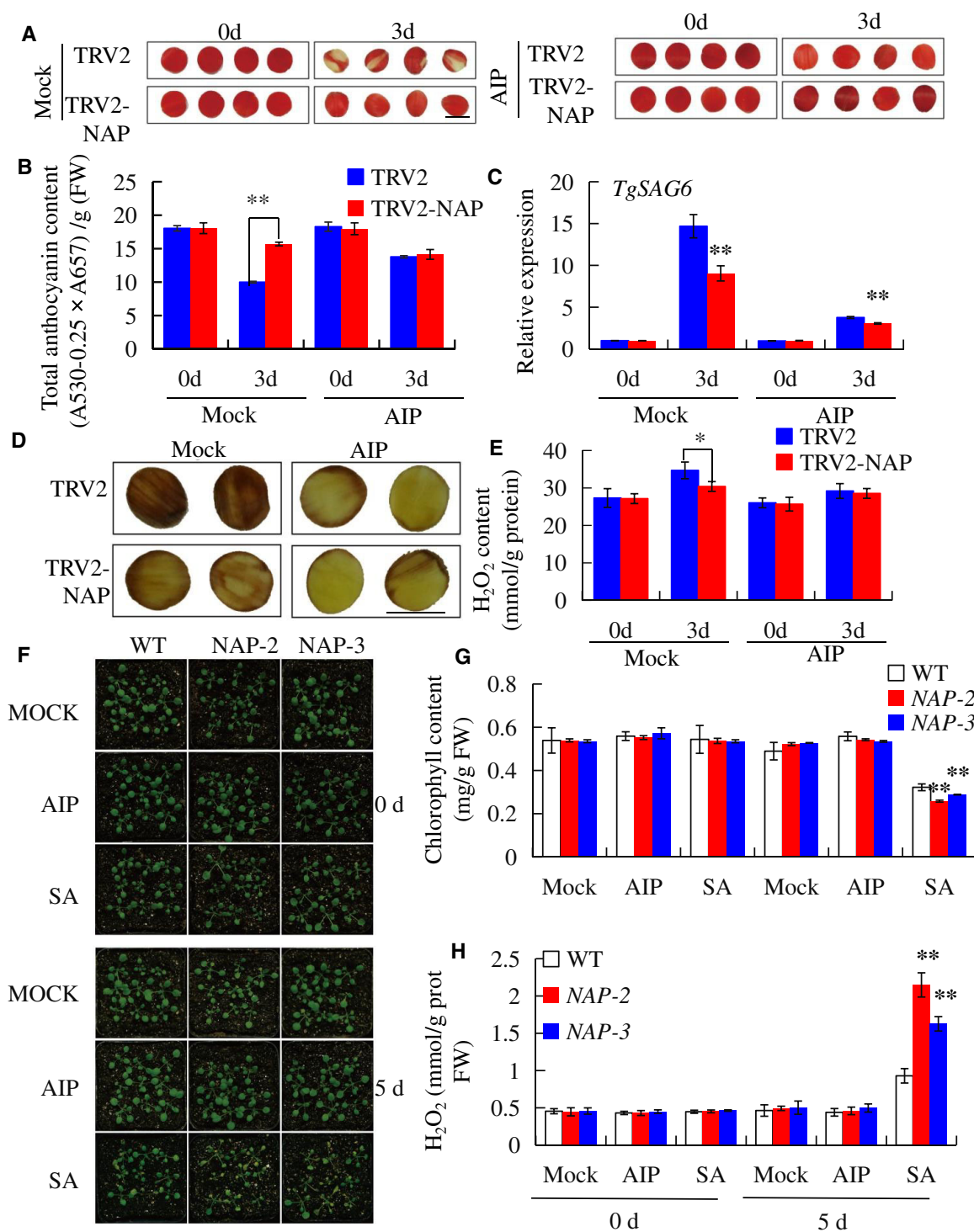
Figure 4 Effects of SA biosynthesis on the senescence of tulip petals and 35S:*TgNAP* transgenic Arabidopsis. A, The phenotypes of *TgNAP*-silenced petals and the TRV control treated with 30 μM AIP. The samples in each boxed area were photographed at the same time. B and C, The total anthocyanin content (B) and expression level of *TgSAG6* (C) of TRV control and *TgNAP*-silenced petals treated with AIP. The expression levels of the samples at the indicated time point were normalized to a *TgUBQ10-like* gene. Relative gene expression was calculated using the $2^{-\Delta\Delta Ct}$ method. Error bars indicate SE ($n = 3$). Asterisks indicate significant difference between WT and two transgenic lines based on the LSD values (**$P < 0.01$). Different letters denote significant differences at $P < 0.05$ analyzed by Tukey's test. D, In situ detection of H_2O_2 in TRV control and *TgNAP*-silenced plants after AIP treatment, as revealed by histochemical staining with DAB. The samples in each boxed area were photographed at the same time and are part of a single image. E, H_2O_2 content in TRV control and *TgNAP*-silenced plants before and after AIP treatment. Error bars indicate SE ($n = 3$). Asterisks indicate significant difference between WT and two transgenic lines based on the LSD values (*$P < 0.05$). F, The phenotypes of 2-week-old WT and transgenic lines (#2 and #3) sprayed with or without 30 μM AIP and 200 μM SA for 5 d. G–I, Measurement of chlorophyll contents (G), DAB staining (H), and H_2O_2 contents (H) in the leaves shown in (F) on Day 5. Error bars indicate SE ($n = 3$). Asterisks indicate significant difference between WT and two transgenic lines based on the LSD values (*$P < 0.05$, **$P < 0.01$). Scale bar, 1.0 cm.

the leaves of *TgNAP*-OE exhibited more yellowish than the leaves of WT (Supplemental Figure S5a). However, AIP treatment could obviously arrest the leaf senescence of *TgNAP*-OE (Supplemental Figure S5a). Consistently, the chlorophyll contents displayed decreased or increased levels after SA and AIP treatment, respectively, in either detected genotypes (Supplemental Figure S5b). Moreover, AIP treatment reduced H_2O_2 accumulation either in WT or in *TgNAP*-OE leaves (Supplemental Figure S5, c and d). Additionally, the whole plants of 2-week-old WT and *TgNAP*-OE transgenic Arabidopsis were also sprayed with AIP and SA. Upon 5 d of SA treatment, *TgNAP*-OE showed a larger portion of yellowing than WT (Figure 4F). Consistent with these phenotypes, the chlorophyll contents were lower and H_2O_2 levels were higher in *TgNAP*-OE transgenic Arabidopsis than WT (Figure 4, G and H). All these data indicated that *TgNAP* promotes plant senescence in an SA- and/or H_2O_2-dependent manner and SA biosynthesis potentially functions upstream of H_2O_2 accumulation in this process.

TgNAP directly activates *TgPAL1* and *TgICS1* expressions

Isochorismate synthase (ICS) and phenylalanine ammonia-lyase (PAL) are two key enzymes in SA biosynthesis pathway, which are responsible for converting branched acid and phenylalanine into isochoric acid and trans-cinnamic acid, respectively (Chen et al., 2009; Dempsey et al., 2011). The promoter sequences of *TgPAL1* and *TgICS1* were cloned and both contain a core NAC-binding element located at −716 ∼−713 bp and −700 ∼−679 bp, respectively (Figure 5A). The binding sequence is very similar to the region of *AtSAG113*, *AtSAG202*, and *AtCKX3* that AtNAP bound to (Zhang and Gan, 2012; Hu et al., 2021; Wang et al., 2022). To explore whether TgNAP directly promotes *TgPAL1* and *TgICS1* expression, yeast-one-hybrid (Y1H) assay was employed using TgNAP protein as the prey (Figure 5B). All transformed yeast grew well on SD/-Leu/-Ura media, whereas only positive control and yeast cells harboring TgNAP prey protein and wild-type TgNAP core binding sequence (PP and PI) survived on media supplemented with Aureobasidin A (AbA; Figure 5C). Electrophoretic mobility shift assay (EMSA) was carried out to document the interactions between TgNAP and core binding sequence. Gel-shift assay indicated His-TgNAP fusion protein is able to bind to the biotin-labeled probes PP and PI containing TgNAP core binding sequence. The protein-DNA complex binding was abolished when His-TgNAP fusion protein was incubated with mutated probes AAAG (mPP and mPI). After adding the unlabeled competitor probes, the binding capacity decreased gradually in a dosage-dependent manner (Figure 5D). These findings suggested that TgNAP directly and specifically binds to the promoter regions of *TgPAL1* and *TgICS1*, respectively. A dual LUC reporter assay was further performed to examine the *in vivo* interactions of TgNAP protein with *TgPAL1* and *TgICS1* promoters in *N. benthamiana* leaves (Figure 5E). Substantial LUC

fluorescence signals were observed in the presence of the TgNAP-SK effector and wild-type PP and PI reporters, whereas very low signals were found for mutated mPP and mPI reporters (Figure 5F). The LUC/REN ratio was significantly higher in co-transformation of TgNAP-SK and reporters containing TgNAP core binding sequence when compared to the control and mutated reporters (Figure 5G). Taken together, these results revealed that TgNAP could activate the *TgPAL1* and *TgICS1* promoter-driven transcription by binding to core-binding motif.

Silencing of *TgNAP* delayed H_2O_2-induced tulip petal senescence

To obtain more insight about the ROS roles during tulip petal senescence, an exogenous treatment of H_2O_2 was performed using the tulip petal discs and Arabidopsis leaves. With 2.0 mM H_2O_2 treatment for 3 d in dark, the senescing phenotypes in TRV control samples including color fading and petal curly were substantially enhanced when compared with control treatment, while TRV2-*TgNAP* petals largely remained fresh and red color (Figure 6A). TRV2-*TgNAP* petals had less H_2O_2 accumulation than TRV2 control based on DAB staining results (Figure 6C). Quantification of H_2O_2 content showed that the levels of H_2O_2 in TRV2 control were significantly higher than that in TRV2-*TgNAP* silenced petal discs with or without H_2O_2 treatment (Figure 6C). The activity of H_2O_2 scavenging enzyme POD increased following petal senescence and was higher in TRV2-*TgNAP* silenced petal discs when compared to TRV2 control (Figure 6D). Consistently, the expression levels of *TgPOD12* and *TgPOD17* were upregulated after *TgNAP* silencing (Figure 6, E and F).

TgNAP promotes H_2O_2-induced senescence

In transgenic Arabidopsis, both detached leaves and whole plants of *TgNAP*-OE lines and WT were used for H_2O_2-induced leaf senescence assays. Leaves of *TgNAP*-OE lines were prone to be senescing and turned yellow earlier than those of WT after H_2O_2 treatment (Supplemental Figure S6, a and e). Quantitative measurement and DAB staining indicated that *TgNAP*-OE lines accumulated higher H_2O_2 content than WT (Supplemental Figure S6, b, d, and g). POD activity decreased in *TgNAP*-OE lines which were consistent with the H_2O_2 levels and leaf phenotype (Supplemental Figure S6, c and f). Additionally, the expression levels of ROS-related genes in transgenic Arabidopsis and WT were investigated. The results showed that the expressions of ROS production-related genes (*AtRBOHA*, *AtRBOHD*, and *AtRBOHF*) showed significant upregulation (Supplemental Figure S7, a–c), while those of ROS scavenging-related genes (*AtPRX4*, *AtPRX33*, and *AtPRX72*) were significantly downregulated (Supplemental Figure S7, d–f). These data indicated that *TgNAP* is a positive regulator in H_2O_2-induced petal or leaf senescence.
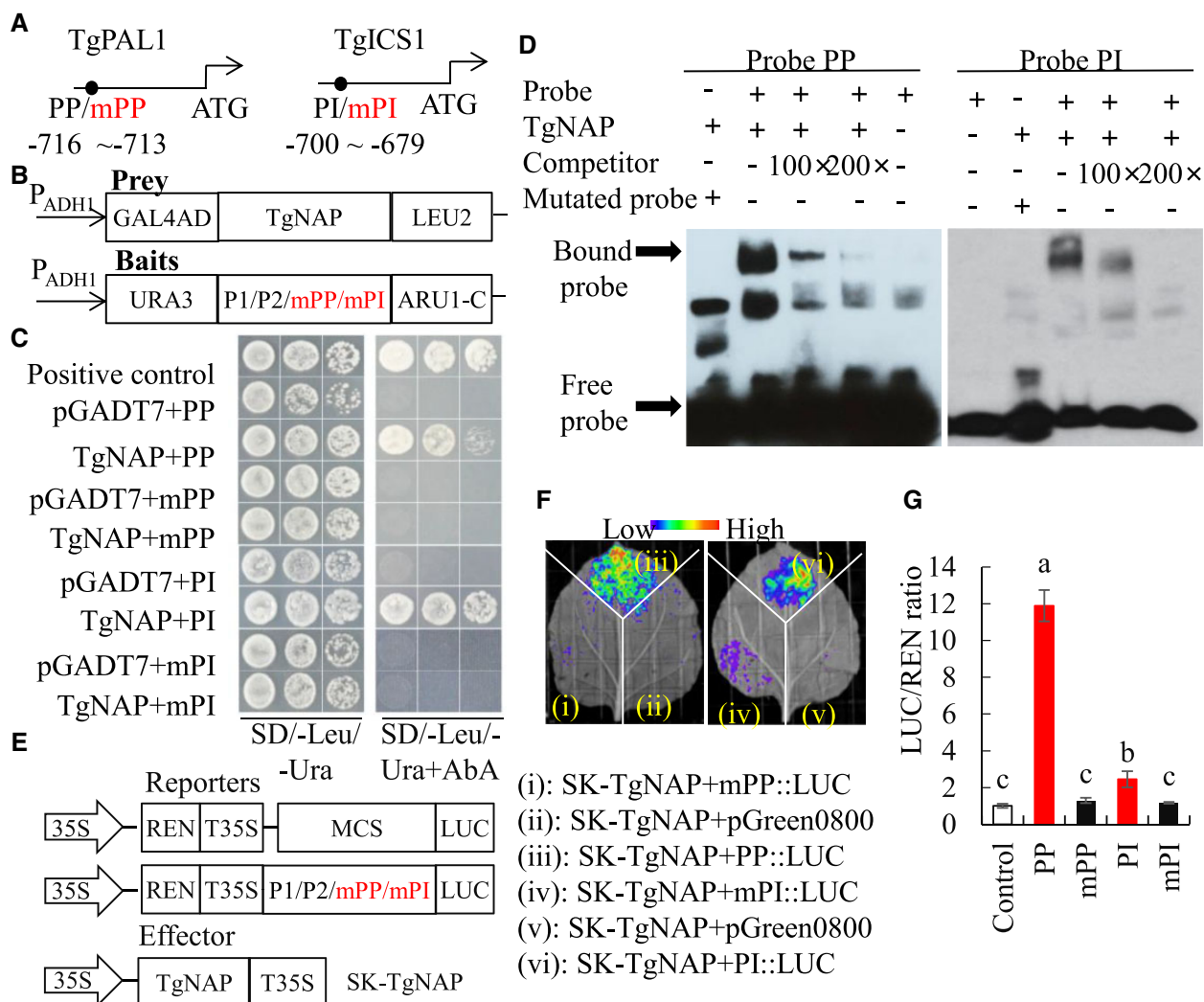
Figure 5 Direct binding of TgNAP to promoters of *TgPAL1* and *TgICS1*. A, Schematic diagram of the *TgPAL1* and *TgICS1* promoter. The black circles indicate the position of the partial promoter fragments within CACG motifs. PP: promoter of *TgPAL1*; PI: promoter of *TgICS1*. The numbers shown below indicated the position of specific binding of TgNAP in the promoters ahead of ATG. B, The prey and bait constructs used for Y1H assay. mPP and mPI is a mutated version of PP and PI, in which the CACG was replaced with AAAG. PADH1, promoter of alcohol dehydrogenase1. GAL4AD, galactose-specific transcription enhancing factor 4 activation domain. C, Growth of yeast cells co-transformed with various prey plus bait combinations on selective medium (SD/-Ura/-Leu) with (right) or without (left) AbA. AbA, Aureobasidin A. Positive control: p53-AbAi + pGAD-p53; Negative control: bait + pGADT7. D, EMSA analysis of specific binding of TgNAP to the promoter of *TgPAL1* and *TgICS1*. The purified His-TgNAP protein and biotin-labeled probe of designed fragments containing CACG motif or mutated AAAG motif were used. Competitor was unlabeled probe at 100- and 200-fold. +: presence; –: absence. E, The schematic of the TgNAP effector and *pTgICS1::LUC*, *pTgPAL1::LUC* reporters. T35S, the terminator of CaMV 35S, respectively. MCS, multiple cloning sites. LUC, firefly luciferase. REN, Renilla luciferase. F, Live image of transcriptional activation of the *TgICS1* and *TgPAL1* promoters by TgNAP in *N. benthamiana* leaves using Dual-LUC system. G, Quantitative analysis of dual-LUC transient expression assays of the promoter activity in *N. benthamiana* protoplasts. LUC/REN ratio of SK-TgNAP + pGreen0800 empty vector was used as the negative control and was considered as 1 for data normalization. Error bars indicate SE ($n = 3$). Different letters denote significant differences at $P < 0.05$ analyzed by Tukey's test.

TgNAP binds to promoters of *TgPOD12* and *TgPOD17* to suppress gene expression

To further investigate the relationship between TgNAP and ROS homeostasis during petal senescence, the promoter sequences of *TgPOD12* and *TgPOD17* were amplified from tulip genomic DNA. There was one core-binding motif in the promoters of *TgPOD12* and *TgPOD17*, respectively (Figure 7A). Y1H was conducted to investigate the interaction between TgNAP and promoters of *TgPOD12*/*TgPOD17*.

The prey and bait vectors were constructed as indicated (Figure 7B). The results showed that only positive control and yeast cells co-transformed with TgNAP-AD prey and the wild-type P1/P2 bait grew normally on media supplemented with AbA. However, when the P1/P2 motif sequence was mutated from CACG to AAAG, the growth of yeast was completely inhibited (Figure 7C). Next, EMSA was performed to verify the binding of TgNAP to *TgPOD12* and *TgPOD17* promoters. Shifted bands were observed when
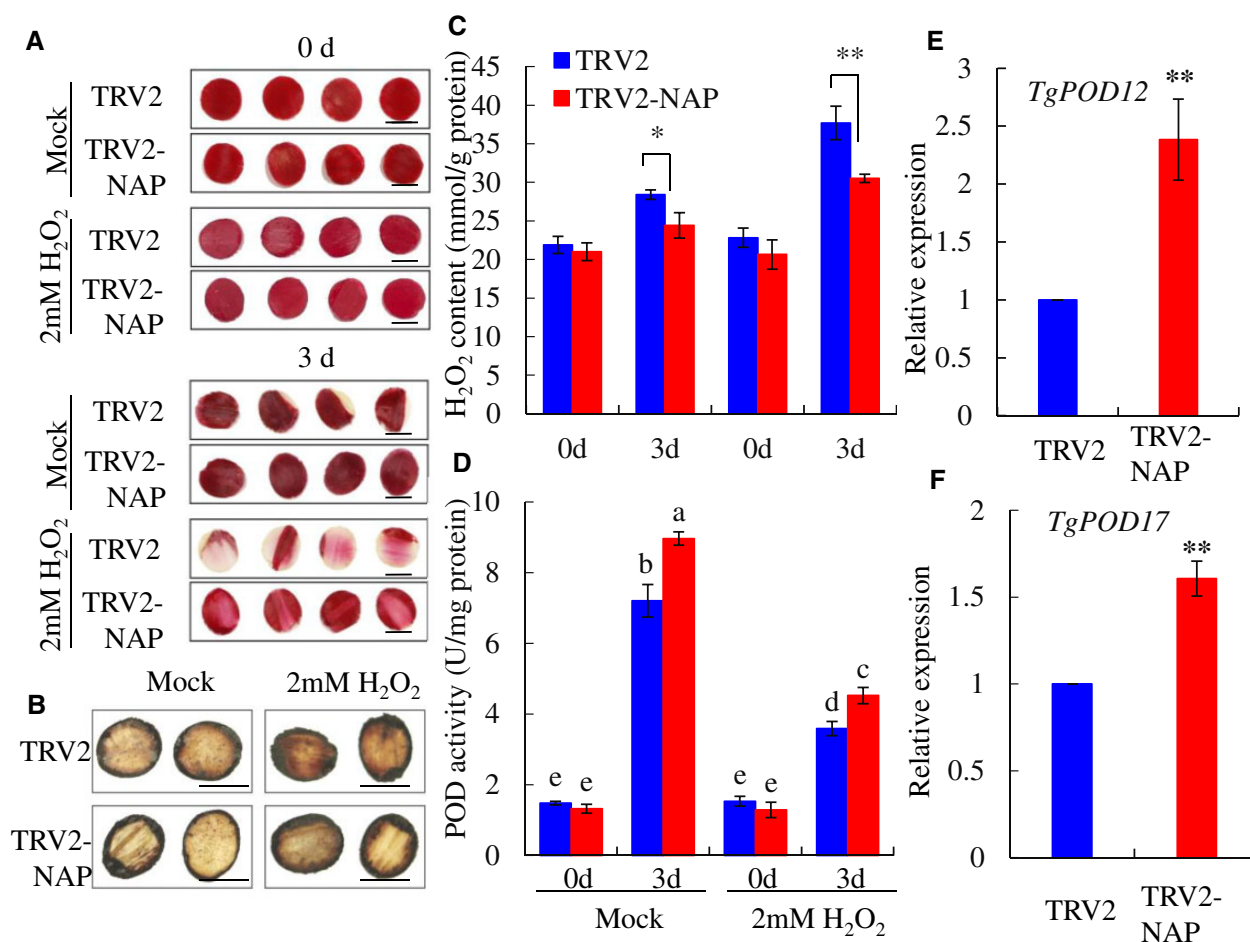
Figure 6 Effect of H_2O_2 on petal senescence in *TgNAP*-silenced and the TRV2 control discs. A, The phenotypes of *TgNAP*-silenced petals and the TRV2 control treated with two mM H_2O_2. The samples in each boxed area were photographed at the same time. B, In situ detection of H_2O_2 in TRV2 control and TgNAP-silenced plants after ddH_2O or H_2O_2 treatment, as revealed by histochemical staining with DAB. The samples in each boxed area were photographed at the same time and are part of a single image. C, The H_2O_2 contents of TRV2 control and *TgNAP*-silenced petals treated with or without two mM H_2O_2. D, The POD enzyme activity levels of TRV2 control and *TgNAP*-silenced petals treat with or without two mM H_2O_2. Blue and red columns indicate the TRV2 control and *TgNAP*-silenced petals, respectively. E and F, Expression levels of TgPOD12 (E) and TgPOD17 (F) in TRV2 control and *TgNAP*-silenced petals. Error bars indicate SE ($n = 3$). Asterisks indicate significant difference between the *TgNAP*-silenced petals and the TRV control based on the LSD values (*$P < 0.05$, **$P < 0.01$). Different letters denote significant differences at $P < 0.05$ analyzed by Tukey's test. Scale bar, 2.0 cm.
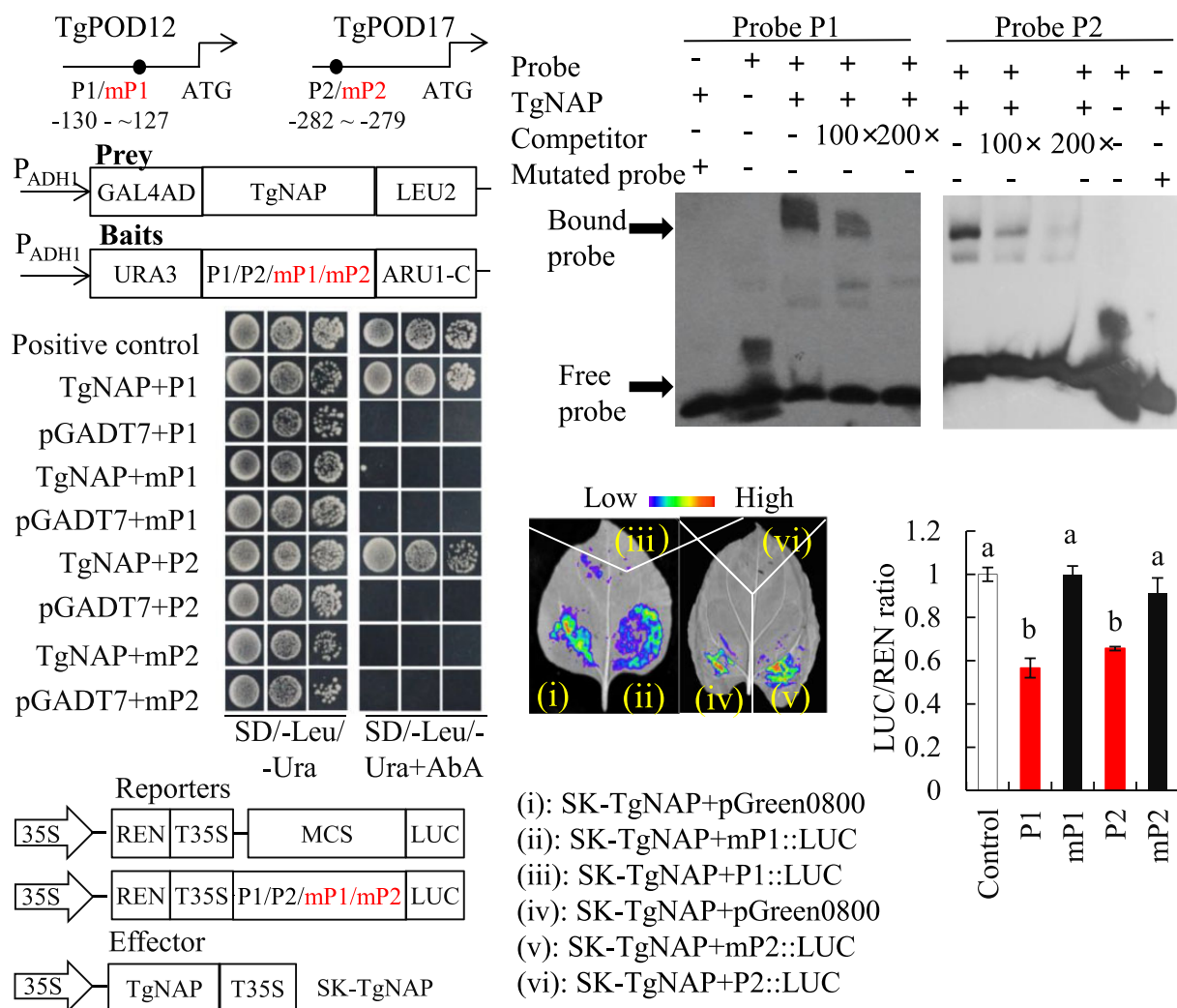
His-TgNAP fusion protein was incubated with the biotin-labeled probes P1 and P2 containing core-binding motif, respectively (Figure 7D). Dual LUC reporter assays were conducted to further verify the transcriptional effect of TgNAP on *TgPOD12* and *TgPOD17* genes. Quantitative measurement of LUC/REN ratio and observation of LUC fluorescence indicated that TgNAP is able to suppress the promoters of *TgPOD12* and *TgPOD17* (Figure 7, E–G). These results were consistent with gene expression level changes of *TgPOD12* and *TgPOD17* in TRV2-*TgNAP* petals (Figure 6, E and F). Taken together, these results reveal that TgNAP represses *TgPOD12* and *TgPOD17* transcription through binding to the core-binding motif.

Discussion

Flower senescence is the terminal step and irreversible process of flower development (van Doorn and Woltering, 2008; Ma et al., 2018). The petals, as the most important organ in flower, are able to attract pollinators and promote pollination (van Doorn and Woltering, 2008; Rogers, 2013; Ma et al., 2018). Petal senescence is accompanied by color fading, wilting, loss of scent, and abscission, that impacts economic and ornamental values of the flower (van Doorn and Woltering, 2008; Rogers, 2013; Ma et al., 2018; Sun et al., 2021). Different from leaf senescence, the molecular mechanisms of flower or petal senescence are much less studied and remain largely elusive (Woo et al., 2013; Bresson et al., 2018).

Previous reports have indicated that NAC TF family is prominent among plant leaf senescence-associated transcriptional regulators. Arabidopsis *AtNAP*, which is most closely related to *TgNAP*, has been demonstrated to cause precocious leaf senescence (Guo and Gan, 2006). Moreover, AtNAP is able to bind the promoter of its target genes

Figure 7 Direct binding of TgNAP to promoters of *TgPOD12* and *TgPOD17*. A, Schematic diagram of the *TgPOD12* and *TgPOD17* promoters. The black circles indicate the position of the partial promoter fragments within CACG motifs. P1: promoter of *TgPOD12*; P2: promoter of *TgPOD17*. B, The prey and bait constructs used for Y1H assay. mP1 and mP2 are mutated versions of P1 and P2, in which the CACG was replaced with AAAG. PADH1, promoter of alcohol dehydrogenase1. GAL4AD, galactose-specific transcription enhancing factor 4 activation domain. C, Growth of yeast cells co-transformed with various prey + bait combinations on selective medium (SD/-Ura/-Leu) with (right) or without (left) AbA. AbA, Aureobasidin A. Positive control: p53-AbAi + pGAD-p53; Negative control: bait + pGADT7. D, EMSA analysis of specific binding of TgNAP to the promoters of TgPOD12 and TgPOD17. The purified His-TgNAP protein and biotin-labeled probe of designed fragments containing CACG motif or mutated AAAG motif were used. Competitor was unlabeled probe at 100- and 200-fold. +: presence; −: absence. E, The schematic of the TgNAP effector and *pTgPOD12::LUC*, *pTgPOD17::LUC* reporters. T35S, the terminator of CaMV 35S, respectively. MCS, multiple cloning sites. LUC, firefly luciferase. REN, Renilla luciferase. F, Live image of transcriptional activation of the *TgPOD12* and *TgPOD17* promoters by TgNAP in *N. benthamiana* leaves using Dual-LUC system. G, Quantitative analysis of dual-LUC transient expression assays of the promoter activity in *N. benthamiana* protoplasts. LUC/REN ratio of SK-TgNAP + pGreen0800 empty vector was used as the negative control and was considered as 1 for data normalization. Error bars indicate SE ($n = 3$). Different letters denote significant differences at $P < 0.05$ analyzed by Tukey's test.

AtSAG113 and *AtCKX3* to mediate ABA and CK pathways to facilitate leaf senescence (Zhang and Gan, 2012; Hu *et al.*, 2021). Rice *OsNAP* was shown to play a positive role in ABA-induced leaf senescence (Mao *et al.*, 2017). Rose RhNAP has been reported to accelerate senescence in mature petals and enhance dehydration tolerance in young rose petals by activating the expression of *RhCKX6* (Zou et al., 2021). Meanwhile, knocked down *GnNAP* in cotton also caused a greatly delay in leaf senescence (Fan et al., 2015). Interestingly, we found that TgNAP promotes tulip petal senescence through activating SA biosynthesis-related genes *TgPAL1* and *TgICS1*, but suppresses expression of antioxidant-related genes *TgPOD12* and *TgPOD17* (Figures 5 and 7). These results are different from what observed by Kim et al. (2018) indicating NAC TFs play dual roles in regulating plant senescence through SA and ROS pathways. In this study, silencing *TgNAP* in tulip greatly delayed senescence process in petal discs (Figure 3), whereas overexpression of *TgNAP* remarkably accelerated leaf senescence in Arabidopsis (Figure S4). These data were consistent with the

results of *TgNAP* putatively orthologous genes from other plant species. All these results revealed that *TgNAP* functioned as a positive regulator during tulip petal senescence.

To date, numerous studies have dissected the different signaling pathways mediated by TFs to regulate senescence process, including SA and H_2O_2 (Guo et al., 2017; Niu et al., 2020; Wang et al., 2020a). In line with this fact, we found that SA and H_2O_2 contents were significantly reduced in TRV2-*TgNAP* petals but increased in *TgNAP*-OE lines (Figure 3; Supplemental Figure S4). H_2O_2 and SA pathways were reported to form an elegant regulatory feedback loop to stimulate each other's accumulation in multiple plant physiological processes including aging and senescence (León et al., 1995; Kauss and Jeblick, 1995; Rao et al., 1997; Guo et al., 2017). Our data showed that supplement with SA synthesis inhibitor AIP could greatly inhibit H_2O_2 accumulation in TRV2-*TgNAP* petals during petal senescence (Figure 4). Meanwhile, SA treatment enhanced H_2O_2 levels whereas AIP treatment reduced H_2O_2 accumulation in *TgNAP* overexpression and WT Arabidopsis (Figure 4). Therefore, SA promotes H_2O_2 production whereas H_2O_2 also elicits SA biosynthesis, confirming the roles of both molecules during tulip petal senescence.

Most TFs function as positive or negative regulators through binding to the cis-acting elements in the promoter of downstream target genes to modulate gene expression. Recently, several TFs were reported to regulate SA and ROS pathways following plant senescence. Arabidopsis AtWRKY75 plays a positive role in promoting leaf senescence through activation of *AtSID2* and repression of *AtCAT2* expression to enhance SA and H_2O_2 accumulation (Guo et al., 2017). AtWRKY42 and AtWRKY55 also participate in SA and ROS pathways to accelerate leaf senescence by activating *AtSID2* and *AtRBOH* genes (Niu et al., 2020; Wang et al., 2020a). In Arabidopsis, ANAC019, ANAC055, and ANAC072 function as positive regulator of plant senescence partially through SA and JA pathways in terms of GO enrichment analysis (Hickman et al., 2013). Previous researches have defined that CACG is one of the core binding motif of NAC TFs (Olsen *et al.*, 2005; Zhang and Gan, 2012; Hu *et al.*, 2021; Wang *et al.*, 2022). We further found that TgNAP could directly bind to the core-binding motif containing CACG in *TgICS1* and *TgPAL1* promoters, which is similar to AtNAP binding motif (Zhang and Gan, 2012; Hu *et al.*, 2021; Wang *et al.*, 2022), to activate their transcription in tulip (Figure 5). Meanwhile, the transcript levels of *TgICS1* and *TgPAL1* and the SA content decreased in the *TgNAP* silenced petal discs (Figure 3, E–G), but increased in *TgNAP* overexpression plants in relative to WT (Supplemental Figure S4, h–l). Our results are in line with a recent report about a positive feedback regulatory loop, SA-AtNAP-SAG202-ICS1-SA, that modulates SA-associated leaf senescence (Wang *et al.*, 2022). However, other Arabidopsis NAC TFs, such as ANAC017, ANAC082, and ANAC090 troika, negatively regulate leaf senescence by suppressing SA and ROS responses (Kim et al., 2018), which was consistent with

our results that exogenous supply of AIP (inhibitor of SA) could retard the senescence of tulip petals and Arabidopsis leaves (Figure 4; Supplemental Figure S5). Consequently, NAC transcription factors play divergent roles in plant senescence depending upon the specific regulation of downstream targets.

Although SA is synthesized from both ICS and PAL pathways, and *TgICS1* and *TgPAL1* are both activated by TgNAP, PAL pathway is responsible for synthesis of roughly 5% of SA in pathogen-infected or UV-treated Arabidopsis (Chen et al., 2009). PAL catalyzes phenylalanine to trans-cinnamate. It is the first step in the phenylpropanoid pathway and a crucial regulation point between primary and secondary metabolism, which eventually generate various phenylpropanoids, including SA and other secondary metabolite, such as flavonoids, lignin, stilbenes, anthocyanins, etc. (Huang et al., 2010; Vogt, 2010; Kong, 2015). Hence, PAL is involved in various signaling pathways to response to environmental stresses, plant growth, and development (Dixon and Paiva, 1995; MacDonald and D'Cunha, 2007; Chen et al., 2009). Therefore, TgNAP probably activates *TgPAL1* to regulate other compounds synthesis, not only SA, which also participates in petal senescence regulation.

ROS plays crucial roles during natural course of senescence, and the accumulation of which is able to trigger senescence (Del Río and López-Huertas, 2016; Rogers and Munné-Bosch, 2016; Singh et al., 2016). As a relatively diffusible and stable ROS molecular, H_2O_2 increases during plant senescence, and the accumulated H_2O_2 resulted in a positive feedback regulation to senescence progress (Vanacker et al., 2006; Khanna-Chopra, 2012). Excessive levels of ROS, especially H_2O_2 content, can cause detrimental damage to cellular components, which lead to accelerated senescence process (Miller et al., 2010; Huang et al., 2016). Thus, antioxidant enzymes, such as CAT, POD, and SOD, are critical players for ROS scavenging to maintain the equilibrium of ROS accumulation (Gill and Tuteja, 2010). In addition to promote SA synthesis, TgNAP was also found to be involved in H_2O_2 accumulation to promote petal senescence in tulip. We discovered that two H_2O_2 scavenging-related genes, *TgPOD12* and *TgPOD17*, were greatly upregulated in *TRV-TgNAP* petals and considerably downregulated in *TgNAP* overexpressed plants (Figure 6, C and D; Supplemental Figure S7). Further analysis revealed that TgNAP could directly recognize and bind to the core-binding motif in *TgPOD12* and *TgPOD17* promoters to repress their expression (Figure 7), and then lead to more ROS accumulation (Figure 6; Supplemental Figure S6). Recently, AtNAC075 was reported to repress *CATALASE 2* (*CAT2*) expression through directly binding to its promoter region to negatively regulate plant senescence (Kan et al., 2021). Moreover, several other NAC TFs such as *JUB1* and *ORS1* are transcriptionally induced by H_2O_2 (Balazadeh et al., 2011; Wu et al., 2012), indicating a complicated regulation between NAC TFs and ROS pathway. These data collectively demonstrated that NAC

TFs regulate plant senescence through integrating internal ROS signals.

Collectively, the expression of *TgNAP* was induced in senescing petals as well as by exogenous SA treatment. In turn, *TgNAP* further promotes the accumulation of SA and H_2O_2, which are closely related (Kauss and Jeblick, 1995; León et al., 1995; Rao et al., 1997), to trigger petal senescence. It is predictable that each of three factors (*TgNAP*, SA, and ROS) mutually activates the other two to initiate and accelerate the petal senescence process. Therefore, we propose that *TgNAP*-SA-ROS feedback loops promote tulip petal senescence in an irreversible manner. Nevertheless, the interactions between SA and H_2O_2 signaling pathways during plant senescence are still not well understood. Even though retarding SA synthesis inhibits intracellular H_2O_2 accumulation in tulip petals, the exact regulation effect of H_2O_2 treatment on SA pathway remains elusive. Further investigation into the core members harboring both SA and ROS homeostasis will be necessary to dissect the senescence mechanism and facilitate prolonging cut flower's vase life.

In conclusion, our study showed that a senescence-associated NAC TF TgNAP from *T. gesneriana* acts as a positive regulator of petal senescence. We propose a work model to illustrate how TgNAP functions in petal senescence in tulip (Figure 8). TgNAP obtains a dual regulation to SA biosynthesis and H_2O_2 accumulation during petal senescence in tulip. It is able to active SA synthesis gene (*TgPAL1* and *TgICS1*) expressions and represses POD-encoding gene (*TgPOD12* and *TgPOD17*) expressions, which resulted in more SA and H_2O_2 accumulation to promote petal and leaf senescence either in tulip or in transgenic Arabidopsis plants. Moreover, a mutual enhancement between SA and H_2O_2 could be responsible for irreversible progress during petal senescence in tulip flowers. The upstream regulator of *TgNAP* and other signaling pathways regulated by TgNAP remains to be investigated in the future.

Materials and methods

Plant materials and growth conditions

Tulipa gesneriana 'World Favorite' were planted in the greenhouse at Huazhong Agricultural University (Wuhan, China) under natural light at 18∼22°C. The flower tissues were sampled at different stages from bud coloring to petal senescence as previously described (Wang et al., 2020b). In previous study, five stages were selected for transcriptome analysis to obtain a comprehensive insight during flower opening and senescence process (RNA seq accession No. GSE136183), including green floral buds (GFB, Stage 1), colored floral buds (CFB, Stage 2), flowers in full bloom (FB, Stage 3), flowers in early senescent phase (ESP, Stage 4), and flowers in late senescent phase (LSP, Stage 5). SA and AIP (an inhibitor of PAL to decrease SA content) were used for petal discs treatments (Solecka and Kacperska, 2013). Intact tulip flower or petal discs (∼1.0 cm²) were placed in 200 µM SA or 30 µM AIP for indicated time courses. Mock samples were treated with distilled water. The *A. thaliana*

ecotype Col-0 was used for transformation. Plants were grown in growth room under 16 h light/8 h dark photoperiod condition. To generate *TgNAP* overexpression lines, the ORF of *TgNAP* was clone into pCAMBIA1300 vector using the *Xba I* and *Spe I* restriction sites. The resulting pCAMBIA1300-*TgNAP* was introduced into *Agrobacterium tumefaciens* strain GV3101 and then transformed into Arabidopsis by flower dip method (Clough and Bent, 1998). *Nicotiana benthamiana* was used for transient transformation for Subcellular location and Dual-LUC assays.

H_2O_2 measurements and DAB staining

H_2O_2 contents were measured using commercial detection kits (Nanjing Jiancheng Bioengineering Institute, China) according to the manufacturer's instructions. In brief, 0.15 g of frozen flower samples were fully ground with 1.5 mL PBS buffer (0.1 mM, pH 7.8) and centrifuged at 4,000 rpm for 20 min at 4°C. And the supernatant was collected and used for H_2O_2 contents analysis. For histochemical staining, samples were incubated in 1 mg/mL DAB solution (in 0.01 mM PBS, pH 3.8) in dark for 10 h and then decolorized in 75% (v/v) ethanol until photographing.

Physiological measurements

Chlorophyll contents were measured as previously described. In brief, the plant leaves were cut and incubated in 95% ethanol for 1 d in dark. The absorbance was measured at 649 and 665 nm by using spectrophotometer. The chlorophyll contents were calculated following a formula as previously described (Tian et al., 2020). For anthocyanin contents measurement, the flower samples were dipped into acidic MeOH solution for 24 h at 4°C. The absorbance was measured at 530 and 657 nm as previously described (Luo et al., 2016; Shen et al., 2019). The total anthocyanin contents were determined according to a specific formula: $Q_{Anthocyanins} = (A_{530} - 0.25 \times A_{657})/M$. For SA measurement, 100 mg of samples were collected and frozen in liquid nitrogen, and SA contents were extracted and determined on UPLC-MS/MS system as previously described (Pan et al., 2010).

Senescence phenotype analysis

For natural leaf senescence, the third and fourth leaves of 28-d-old seedlings were used for chlorophyll content analysis and detection of gene expression. For H_2O_2-induced detached leaf senescence, seventh to eighth rosette leaves were detached and put in MES buffer (2 mM, pH 5.8) with or without 2 mM H_2O_2 for 3 d. For H_2O_2 induced seedlings senescence, 2-week-old Arabidopsis grown in soil separated with or without 200 mM H_2O_2 for 5 d under 16 h light/8 h dark photoperiod condition. For SA and AIP treatment, seventh to eighth rosette leaves were detached and incubated in MES buffer (2 mM, pH 5.8) with 200 µM SA or 30 µM AIP for 3 d, 2-week-old Arabidopsis grown in soil separated with or without 200 µM SA or 30 µM AIP for 5 d under 16 h light/8 h dark photoperiod condition. For VIGS samples, the phenotypes of petal discs were observed daily until
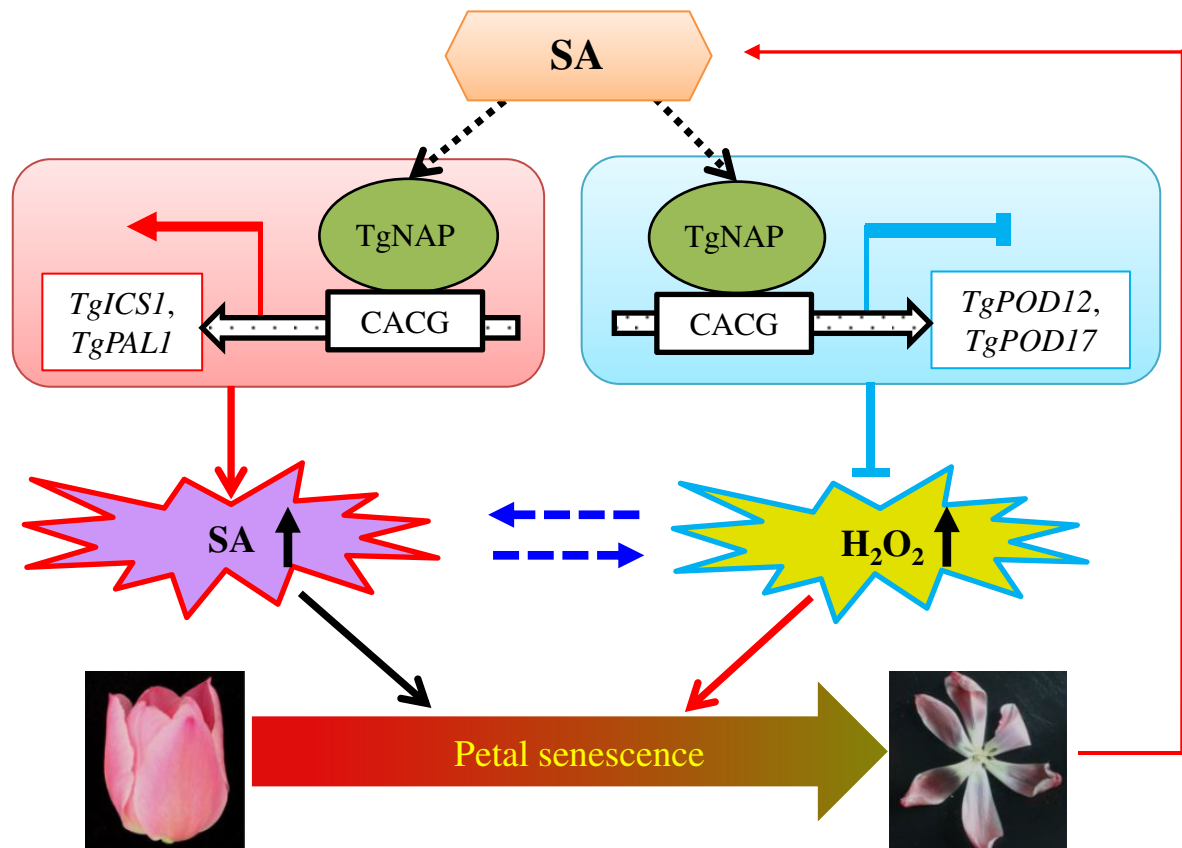
Figure 8 A proposed working model for the regulatory network of *TgNAP* during tulip petal senescence. *TgNAP* is induced by petal senescence and exogenous SA treatment, which subsequently activates *TgICS1* and *TgPAL1* transcription to enhance SA accumulation. In parallel, H_2O_2 scavenging genes *TgPOD12* and *TgPOD17* are repressed by *TgNAP* resulting in increasing ROS levels. Finally, SA and H_2O_2 work together to accelerate petal senescence in tulip.

senescence and color fading were occurred. For AIP treatment, petal discs were put in distilled water with or without 30 μM AIP. For H_2O_2 treatment, petal discs were incubated in distilled water with or without 2 mM H_2O_2 for 3 d in dark.

RNA extraction and RT-qPCR analysis

Total RNA was extracted from tulip flower and Arabidopsis leaves using commercial RNA purification kit (Aidlab, RN33, China). One microgram of RNA was used for reverse transcription to generate cDNA by using the First Strand cDNA Synthesis Kit (Toyobo, Japan) based on instruction manual. RT-qPCR was performed on a QuantStudio 7 Flex PCR machine (Thermo Fisher Scientific, Inc., Carlsbad, CA, USA) using ChamQ Universal SYBR qPCR Master Mix (Vazyme). The 20 μL reaction mixture contained 10 μL 2 × ChamQ Universal SYBR qPCR Master Mix, 200 ng cDNA, 0.2 μM forward and reverse primers. *TgUBQ10-like* was served as the internal reference gene (Wang et al., 2020b). All primer sequences were listed in Supplemental Table S1. The reaction program was 95°C for 3 min, 40 cycles of 10 s at 95°C and 30 s at 60°C, followed by 95°C for 15 s, 60°C for 60 s, and 95°C for 15 s. Relative gene expression levels were analyzed by $2^{-\Delta\Delta Ct}$ method (Livak and Schmittgen, 2001).

RNA sequencing analysis

cDNA library was generated using the NEBNext Ultra II RNA Library Prep Kit (NEB, USA) and sequenced using an Illumina HiSeq 4000 sequencing system (Illumina, USA) with the paired-end sequencing method. The raw reads were filtered and clean data were mapped to the assembled tulip PacBio full-length transcriptome with the accession number PRJNA703083. Fragments per kilobase of transcript per million (FPKM) were used for the quantification of gene expression. Differential expression changes from three biological replicates were analyzed using the DESeq R package (1.10.1). Genes with FDR $\leqslant$ 0.05 and log2 |fold change| $\geqslant 1$ were assigned as significantly differential expressed genes.

Cluster and protein interaction network analyses

Cluster analysis was conducted using the CLUSTER program (http://bonsai.hgc.jp/~mdehoon/software/cluster/software.htm) with uncentered matrix and complete linkage method (de Hoon et al., 2004). The resulting tree figure was visualized using Java Treeview (http://jtreeview.sourceforge.net/) as previously described (Chan, 2012).

    Protein interaction networks were analyzed using the STRING version 10.5 (https://string-db.org/; Szklarczyk et al., 2015). The resulting data were imported into CytoScape

software (https://cytoscape.org/) to generate protein interaction networks.

Cloning and sequence analysis of *TgNAP*

The full length of *TgNAP* was amplified by using specifically designed primers based on previous transcriptome data of *T. gesneriana* (GSE136183). Homologous proteins from other species were searched and obtained from NCBI database. A phylogenetic tree between TgNAP and all Arabidopsis NAC proteins was constructed using MEGA 7.0 software with neighbor-joining method. Multiple sequence alignment results were shown in GENEDOC software.

Subcellular location of *TgNAP*

The ORF of *TgNAP* without stop codon was amplified and fused to the 101LYFP vector, and the fused plasmid NAP-YFP was transformed into *A. tumefaciens* strain GV3101. For transient transformation, *N. benthamiana* leaves were infiltrated with GV3101 carrying NAP-YFP fused vector or empty vector (YFP) as previously described (Geng and Liu, 2018), and VirD2NLS inserted into mCherry was used as a nuclear marker. YFP signal (excitation at 514 nm, scanning at 520–540 nm) and RFP signal (excitation at 552 nm, scanning at 590–640 nm) were observed by a confocal laser scanning microscope (Leica TCSSP8, Germany).

Transcriptional activation activity assay

For transcriptional activation analysis, the full length of *TgNAP* and two truncated fragments, F1 (1–132 aa) and F2 (133–270 aa), were amplified and cloned into pGBKT7 vector to fuse with GAL4 DNA-binding domain. All resulting plasmids were introduced into yeast strain AH109 according to manufacturer's protocol. The transformed yeast cells were plated onto SD/-Trp medium and SD/-Trp/-His/-Ade medium with or without 4 mg/mL X-α-gal at 30°C for 48–72 h. The transformed yeast with pGBKT7-p53 and empty vector pGBKT7 were used as positive control and negative control, respectively.

VIGS assay in tulip petals

To silence *TgNAP* in tulip petals, a non-conserved fragment of *TgNAP* with 330 bp length located at 425~754 bp downstream of start codon (ATG) was amplified and inserted into pTRV2 vector. The specificity of target region in VIGS assay was verified by sequence alignment. The fused pTRV2-*TgNAP* vector, empty pTRV1 and pTRV2 were individually introduced into *A. tumefaciens* GV3101. The bacterial suspensions containing pTRV2-*TgNAP* and pTRV1, or pTRV2 and pTRV1 were prepared for transformation of tulip petals as previously described (Wu et al., 2017; Wang et al., 2020b). In brief, the pTRV1 bacterial suspension ($OD_{600}=1.5$) was mixed with pTRV2 or pTRV2-*TgNAP* in 1:1 ratio (v/v) and suspended in MES buffer (200 mM acetosyringone, 10 mM $MgCl_2$, and 10 mM MES, pH 5.8). The mixtures of bacterial solutions were incubated in dark at 28°C for 3~4 h. 1.0 cm diameter discs of tulip petals were vacuum-infiltrated in bacterial solutions at 0.7 MPa. The infiltrated discs were washed

with distilled water and incubated in darkness at 8°C for first 3 d, and then were transferred to growth chamber (16 h light/8 h dark) for phenotype observation (Wu et al., 2017). At least 20 tulip tepals were used for each treatment.

EMSA assay

The coding sequence of *TgNAP* was cloned into pHMGWA vector which contains a His tag, and the resulting plasmid was transformed into *Escherichia coli* strain Rosetta (DE3) to generate the His-TgNAP fusion protein. After induction by IPTG (0.5 mM) and expression at 37°C for 3 h, the HIS-TgNAP fusion protein was purified. The His-TgNAP fusion protein was induced by IPTG (0.5 mM) at 37°C for 3 h and purified using Qiagen Ni-NTA Agarose kit. The 40-bp promoter fragments of *TgPAL1*, *TgICS1*, *TgPOD12*, and *TgPOD17* were synthesized as probes with biotin-label at the 3'-end. Competitors were unlabeled DNA with same sequence. The mutant probes were labeled, in which the core binding elements changed from CACG to AAAG. The EMSA assay was conducted using the LightShift Chemiluminescent EMSA Kit (Thermo) following the methods previously described (Geng and Liu, 2018).

Yeast one-hybrid (Y1H) assay

The promoter fragments of *TgPAL1*, *TgICS1*, *TgPOD12*, and *TgPOD17*, which contain CACG, were amplified and fused to pAbAi vector as baits vectors. In addition, mutant baits were created by replacing CACG with AAAG. All resulting bait and mutant bait plasmids were linearized and transformed into Y1H Gold yeast strain. The full length of *TgNAP* was amplified and inserted into pGADT7 to generate prey vector. The prey vector was transformed into bait and mutant bait yeast strains. The transformed yeast clones were spotted on SD/-Leu/-Ura medium with or without AbA. The yeast strains harboring baits and empty pGADT7 vector were used as negative control, whereas the yeast strains harboring pAbAi-p53 and pGADT7-p53 were used as positive control.

Dual-LUC assays

The CDS of *TgNAP* was amplified and cloned into pGreen II 62-SK vector to act as effector. The promoter original and mutated sequences of *TgPAL1*, *TgICS1*, *TgPOD12*, and *TgPOD17* were amplified and cloned into pGreen II 0800-LUC vector to be used as reporters. All of the effector and reporters were introduced into *A. tumefaciens* strain GV3101 and transiently expressed in *N. benthamiana* leaves as previously described (Hu et al., 2018; Wang et al., 2019). The activities of LUC and REN were determined by using the Dual-Luciferase® Reporter Assay System (Promega, USA) following the instructions. For observation of LUC fluorescence, 1 mM D-Luciferin solution was used to spray on the infiltrated leaves that then were placed in dark for 5 min. After darkness, the luminescence was detected under a cooled CCD camera by plant living imaging system (Nightshade LB 985, Germany).

Statistical analysis

All experiments were performed at least twice with triplicate. All data were presented as means ± SE. Student's *t* test and ANOVA were used for statistical difference analysis, and significant level was defined as $P < 0.05$ (*), $P < 0.01$ (**).

Accession numbers

Sequence data from this article can be found in the GenBank/EMBL data libraries under the following accession numbers: AtSAG12 (AT3G20770), AtSAG13 (AT2G29350), AtSID2 (AT1G74710), AtPAL1 (AT2G37040), AtEPS1 (AT5G67160), AtEDS5 (AT4G39030), AtRbohA (AT5G07390), AtRbohD (AT5G47910), AtRbohF (AT1G64060), AtPrx33 (AT3G49110), AtPrx4 (AT1G14540), AtPrx72 (AT5G66390), TgNAP and RNA seq accession No. GSE136183.

Supplemental data

The following materials are available in the online version of this article.

Supplemental Figure S1. RNA sequencing analysis and gene expression profiles during petal senescence of *T. gesneriana*.

Supplemental Figure S2. Phylogenetic tree analysis and multiple alignments of NACs from diverse plants.

Supplemental Figure S3. Silencing of *TgNAP* delayed flower senescence.

Supplemental Figure S4. Overexpression of *TgNAP* promoted leaf senescence in Arabidopsis.

Supplemental Figure S5. Effect of exogenous SA on the senescence of *TgNAP* transgenic Arabidopsis and WT.

Supplemental Figure S6. Effect of exogenous H_2O_2 treatment on *TgNAP* transgenic Arabidopsis and WT.

Supplemental Figure S7. Expression of ROS-related genes in *TgNAP* transgenic Arabidopsis and WT analyzed by RT-qPCR.

Supplemental Table S1. Significantly changed unigenes during five senescence stages of tulip petal.

Supplemental Table S2. Significantly changed unigenes during S4 and S5 senescence stages in tulip petal.

Supplemental Table S3. FPKM values of *TgNACs* from transcriptome data.

Supplemental Table S4. List of all primer sequences used in this study.

Data availability statement

Tulip petal RNA-seq data at five different developmental stages were deposited into NCBI GEO database with the accession number GSE136183. The sequence of *TgNAP* was submitted to NCBI GenBank with the accession number MK239329.

References

Balazadeh S, Kwasniewski M, Caldana C, Mehrnia M, Zanor MI, Xue GP, Mueller-Roeber B (2011) ORS1, an H_2O_2-responsive NAC transcription factor, controls senescence in *Arabidopsis thaliana*. Mol Plant **4**: 346–360

Balazadeh S, Siddiqui H, Allu AD, Matallana-Ramirez LP, Caldana C, Mehrnia M, Zanor MI, Köhler B, Mueller-Roeber B (2010) A gene regulatory network controlled by the NAC transcription factor ANAC092/AtNAC2/ORE1 during salt-promoted senescence. Plant J **62**: 250–264

Bresson J, Bieker S, Riester L, Doll J, Zentgraf U (2018) A guideline for leaf senescence analyses: From quantification to physiological and molecular investigations. J Exp Bot **69**: 769–786

Chan Z (2012) Expression profiling of ABA pathway transcripts indicates crosstalk between abiotic and biotic stress responses in Arabidopsis. Genomics **100**: 110–115

Chen L, Xiang S, Chen Y, Li D, Yu D (2017) Arabidopsis WRKY45 interacts with the DELLA Protein RGL1 to positively regulate age-triggered leaf senescence. Mol Plant **10**: 1174–1189

Chen Z, Silva H, Klessig DF (1993) Active oxygen species in the induction of plant systemic acquired resistance by salicylic acid. Science **262**: 1883–1886

Chen Z, Zheng Z, Huang J, Lai Z, Fan B (2009) Biosynthesis of salicylic acid in plants. Plant Signal Behav **4**: 493–496

Clough SJ, Bent AF (1998) Floral dip: a simplified method for Agrobacterium-mediated transformation of *Arabidopsis thaliana*. Plant J **16**: 735–743

Delessert C, Kazan K, Wilson IW, Van Der Straeten D, Manners J, Dennis ES, Dolferus R (2005) The transcription factor ATAF2 represses the expression of pathogenesis-related genes in Arabidopsis. Plant J **43**: 745–757

Del Río LA, López-Huertas E (2016) ROS generation in peroxisomes and its role in cell signaling. Plant Cell Physiol **57**: 1364–1376

Dempsey DA, Vlot AC, Wildermuth MC, Klessig DF (2011) Salicylic acid biosynthesis and metabolism. Arabidopsis Book **9**: e0156

de Hoon MJ, Imoto S, Nolan J, Miyano S (2004) Open source clustering software. Bioinformatics **20**: 1453–1454

Dixon RA, Paiva NL (1995) Stress-induced phenylpropanoid metabolism. Plant Cell **7**: 1085–1097

Fan K, Bibi N, Gan S, Li F, Yuan S, Ni M, Wang M, Shen H, Wang X (2015) A novel NAP member GhNAP is involved in leaf senescence in *Gossypium hirsutum*. J Exp Bot **66**: 4669–4682

Gan S, Amasino RM (1997) Making sense of senescence. Plant Physiol **113**: 313–319

Geng J, Liu JH (2018) The transcription factor CsbHLH18 of sweet orange functions in modulation of cold tolerance and homeostasis of reactive oxygen species by regulating the antioxidant gene. J Exp Bot **69**: 2677–2692

Gill SS, Tuteja N (2010) Reactive oxygen species and antioxidant machinery in abiotic stress tolerance in crop plants. Plant Physiol Biochem **48**: 909–930

Guo P, Li Z, Huang P, Li B, Fang S, Chu J, Guo H (2017) A tripartite amplification loop involving the transcription factor WRKY75, salicylic acid, and reactive oxygen species accelerates leaf senescence. Plant Cell **29**: 2854–2870

Guo Y, Gan S (2006) AtNAP, a NAC family transcription factor, has an important role in leaf senescence. Plant J **46**: 601–612

Han Y, Chaouch S, Mhamdi A, Queval G, Zechmann B, Noctor G (2013) Functional analysis of Arabidopsis mutants points to novel roles for glutathione in coupling H_2O_2 to activation of salicylic acid accumulation and signaling. Antioxid Redox Sign **18**: 2106–2121

He Y, Fukushige H, Hildebrand DF, Gan S (2002) Evidence supporting a role of jasmonic acid in Arabidopsis leaf senescence. Plant Physiol **128**: 876–884

Hickman R, Hill C, Penfold CA, Breeze E, Bowden L, Moore JD, Zhang P, Jackson A, Cooke E, Bewicke-Copley F, et al. (2013) A local regulatory network around three NAC transcription factors in stress responses and senescence in Arabidopsis leaves. Plant J **75**: 26–39

Huang J, Gu M, Lai Z, Fan B, Shi K, Zhou YH, Yu JQ, Chen Z (2010) Functional analysis of the Arabidopsis *PAL* gene family in plant growth, development, and response to environmental stress. Plant Physiol **153**: 1526–1538

Hu Q, Zhu L, Zhang X, Guan Q, Xiao S, Min L, Zhang X (2018) GhCPK33 negatively regulates defense against *Verticillium dahliae* by phosphorylating GhOPR31. Plant Physiol **178**: 876–889

Huang S, Aken O, Van Schwarzländer M, Belt K, Millar AH (2016) The roles of mitochondrial reactive oxygen species in cellular signaling and stress response in plants. Plant Physiol **171**: 1551–1559

Hu Y, Liu B, Ren H, Chen L, Watkins CB, Gan S (2021). The leaf senescence-promoting transcription factor AtNAP activates its direct target gene CYTOKININ OXIDASE 3 to facilitate senescence processes by degrading cytokinins. Mol Hortic **1**: 1–12

Jimenez A, Creissen G, Kular B, Firmin J, Robinson S, Verhoeyen M, Mullineaux P (2002) Changes in oxidative processes and components of the antioxidant system during tomato fruit ripening. Planta **214**: 751–758

Kan C, Zhang Y, Wang HL, Shen Y, Xia X, Guo H, Li Z (2021) Transcription factor NAC075 delays leaf senescence by deterring reactive oxygen species accumulation in Arabidopsis. Front Plant Sci **12**: 1–11

Kauss H, Jeblick W (1995) Pretreatment of parsley suspension cultures with salicylic acid enhances spontaneous and elicited production of H_2O_2. Plant Physiol **108**: 1171–1178

Khanna-Chopra R (2012) Leaf senescence and abiotic stresses share reactive oxygen species-mediated chloroplast degradation. Protoplasma **249**: 469–481

Kim HJ, Park JH, Kim JJ, Kim JJ, Hong S, Kim J, Kim JH, Woo HR, Hyeon C, Lim PO, et al. (2018) Time-evolving genetic networks reveal a NAC troika that negatively regulates leaf senescence in Arabidopsis. Proc Natl Acad Sci USA **115**: E4930–E4939

Kim YS, Sakuraba Y, Han SH, Yoo SC, Paek NC (2013) Mutation of the Arabidopsis NAC016 transcription factor delays leaf senescence. Plant Cell Physiol **54**: 1660–1672

Kong JQ (2015) Phenylalanine ammonia-lyase, a key component used for phenylpropanoids production by metabolic engineering. RSC Adv **5**: 62587–62603

Lee JH, Park YJ, Kim JY, Park CM (2021) Phytochrome B conveys low ambient temperature cues to the ethylene-mediated leaf senescence in Arabidopsis. Plant Cell Physiol **63**: 326–339

León J, Lawton MA, Raskin I (1995) Hydrogen peroxide stimulates salicylic acid biosynthesis in tobacco. Plant Physiol **108**: 1673–1678

Li Y, Chang Y, Zhao C, Yang H, Ren D (2016) Expression of the inactive *ZmMEK1* induces salicylic acid accumulation and salicylic acid-dependent leaf senescence. J Integr Plant Biol **58**: 724–736

Livak KJ, Schmittgen TD (2001) Analysis of relative gene expression data using real-time quantitative PCR and the $2^{-\Delta\Delta CT}$ method. Methods **25**: 402–408

Lü P, Zhang C, Liu J, Liu X, Jiang G, Jiang X, Khan MA, Wang L, Hong B, Gao J (2014) RhHB1 mediates the antagonism of gibberellins to ABA and ethylene during rose (*Rosa hybrida*) petal senescence. Plant J **78**: 578–590

Luo P, Ning G, Wang Z, Shen Y, Jin H, Li P et al. (2016) Disequilibrium of flavonol synthase and dihydroflavonol-4-reductase expression associated tightly to white vs. Red color flower formation in plants. Front Plant Sci **6**: 1–12

Ma N, Ma C, Liu Y, Shahid MO, Wang C, Gao J (2018) Petal senescence: a hormone view. J Exp Bot **69**: 719–732

Ma X, Zhang Y, Turečková V, Xue GP, Fernie AR, Mueller-Roeber B, Balazadeh S (2018) The NAC transcription factor SLNAP2 regulates leaf senescence and fruit yield in tomato. Plant Physiol **177**: 1286–1302

MacDonald MJ, D'Cunha GB (2007) A modern view of phenylalanine ammonia lyase. Biochem Cell Biol **85**: 273–282

Mao C, Lu S, Lv B, Zhang B, Shen J, He J, Luo L, Xi D, Chen X, Ming F (2017) A rice nac transcription factor promotes leaf senescence via ABA biosynthesis. Plant Physiol **174**: 1747–1763

Mhamdi A, Van Breusegem F (2018) Reactive oxygen species in plant development. Development **145**: dev164376

Miller G, Suzuki N, Ciftci-Yilmaz S, Mittler R (2010) Reactive oxygen species homeostasis and signalling during drought and salinity stresses. Plant Cell Environ **33**: 453–467

Morris K, Mackerness SAH, Page T, Fred John C, Murphy AM, Carr JP, et al. (2000) Salicylic acid has a role in regulating gene expression during leaf senescence. Plant J **23**: 677–685

Nagahage ISP, Sakamoto S, Nagano M, Ishikawa T, Mitsuda N, Kawai-Yamada M, Yamaguchi M (2020) An Arabidopsis NAC domain transcription factor, ATAF2, promotes age-dependent and dark-induced leaf senescence. Plant Physiol **170**: 299–308

Niu F, Cui X, Zhao P, Sun M, Yang B, Deyholos MK et al. (2020) WRKY42 transcription factor positively regulates leaf senescence through modulating SA and ROS synthesis in *Arabidopsis thaliana*. Plant J **104**: 171–184

Oh SK, Lee S, Yu SH, Choi D (2005) Expression of a novel NAC domain-containing transcription factor (CaNAC1) is preferentially associated with incompatible interactions between chili pepper and pathogens. Planta **222**: 876–887

Olsen AN, Ernst HA, Leggio LL, Skriver K (2005) NAC transcription factors: structurally distinct, functionally diverse. Trends Plant Sci **10**: 79-87

Pan X, Welti R, Wang X (2010) Quantitative analysis of major plant hormones in crude plant extracts by high-performance liquid chromatography-mass spectrometry. Nat Protocols **5**: 986–992

Pyung OL, Hyo JK, Hong GN (2007) Leaf senescence. Ann Rev Plant Biol **58**: 115–136

Qiu K, Li Z, Yang Z, Chen J, Wu S, Zhu X, Gao S, Gao J, Ren G, Kuai B, et al. (2015) EIN3 and ORE1 accelerate degreening during ethylene-mediated leaf senescence by directly activating chlorophyll catabolic genes in Arabidopsis. PLoS Genet **11**: 1–20

Rao MV, Paliyath G, Ormrod DP, Murr DP, Watkins CB (1997) Influence of salicylic acid on H_2O_2 production, oxidative stress, and H_2O_2-metabolizing enzymes (salicylic acid-mediated oxidative damage requires H_2O_2). Plant Physiol **115**: 137–149

Rivas-San Vicente M, Plasencia J (2011) Salicylic acid beyond defence: Its role in plant growth and development. J Exp Bot **62**: 3321–3338

Rogers H, Munné-Bosch S (2016) Production and scavenging of reactive oxygen species and redox signaling during leaf and flower senescence: Similar but different. Plant Physiol **171**: 1560–1568

Rogers HJ (2013) From models to ornamentals: how is flower senescence regulated? Plant Mol Biol **82**: 563–574

Schippers JHM, Schmidt R, Wagstaff C, Jing HC (2015) Living to die and dying to live: The survival strategy behind leaf senescence. Plant Physiol **169**: 914–930

Shen Y, Sun T, Pan Q, Anupol N, Chen H, Shi J, Liu F, Deqiang D, Wang C, Zhao J, et al. (2019) RrMYB5- and RrMYB10-regulated flavonoid biosynthesis plays a pivotal role in feedback loop responding to wounding and oxidation in *Rosa rugosa*. Plant Biotechnol J **17**: 2078–2095

Singh R, Singh S, Parihar P, Mishra RK, Tripathi DK, Singh VP, Chauhan DK, Prasad SM (2016) Reactive oxygen species (ROS):

beneficial companions of plants' developmental processes. Front Plant Sci, 7: 1–19

Solecka D, Kacperska A (2013) Phenylpropanoid deficiency affects the course of plant acclimation to cold. Plant Physiol 119: 253–262

Song Y, Yang C, Gao S, Zhang W, Li L, Kuai B (2014) Age-triggered and dark-induced leaf senescence require the bHLH transcription factors PIF3, 4, and 5. Mol Plant 7: 1776–1787

Sun X, Qin M, Yu Q, Huang Z, Xiao Y, Li Y, Ma N, Gao JP (2021) Molecular understanding of postharvest flower opening and senescence. Mol Hortic 1: 1–12

Szklarczyk D, Franceschini A, Wyder S, Forslund K, Heller D, Huerta-Cepas J, Simonovic M, Roth A, Santos A, Tsafou KP, et al. (2015) STRING v10: protein-protein interaction networks integrated over the tree of life. Nucleic Acids Res 43: D447–D452

Tian T, Ma L, Liu Y, Xu D, Chen Q, Li G (2020) Arabidopsis FAR-RED ELONGATED HYPOCOTYL3 integrates age and light signals to negatively regulate leaf senescence. Plant Cell 32: 1574–1588

Tripathi SK, Tuteja N (2007) Integrated signaling in flower senescence: an overview. Plant Signal Behav 2: 437–445

Vanacker H, Sandalio LM, Jiménez A, Palma JM, Corpas FJ, Meseguer V, Gómez M, Sevilla F, Leterrier M, Foyer CH, et al. (2006) Roles for redox regulation in leaf senescence of pea plants grown on different sources of nitrogen nutrition. J Exp Bot 57: 1735–1745

van Doorn WG, Woltering EJ (2008) Physiology and molecular biology of petal senescence. J Exp Bot 59: 453–480

Vlot AC, Dempsey DA, Klessig DF (2009). Salicylic acid, a multifaceted hormone to combat disease. Annu Rev Phytopathol 47: 177–206

Vogelmann K, Drechsel G, Bergler J, et al. (2012) Early senescence and cell death in Arabidopsis saul1 mutants involves the PAD4-dependent salicylic acid pathway. Plant Physiol 159: 1477–1487

Vogt T (2010) Phenylpropanoid biosynthesis. Mol Plant 3: 2–20

Wang C, Dai S, Zhang ZL, Lao W, Wang R, Meng X, Zhou X (2021a) Ethylene and salicylic acid synergistically accelerate leaf senescence in Arabidopsis. J Integr Plant Biol 63: 828–833

Wang M, Dai W, Du J, Ming R, Dahro B, Liu JH (2019) ERF109 of trifoliate orange (Poncirus trifoliata (L.) Raf.) contributes to cold tolerance by directly regulating expression of Prx1 involved in antioxidative process. Plant Biotechnol J 17: 1316–1332

Wang Y, Cui X, Yang B, Xu S, Wei X, Zhao P, Niu F, Sun M, Wang C, Cheng H, et al. (2020a) WRKY55 transcription factor positively regulates leaf senescence and the defense response by modulating the transcription of genes implicated in the biosynthesis of reactive oxygen species and salicylic acid in Arabidopsis. Development 147, dev189647

Wang Y, Liu B, Hu Y, Gan S (2022) A positive feedback regulatory loop, SA- biosynthesis involved in leaf senescence but not defense response. Mol Hortic 2: 1–15

Wang Y, Zhao H, Liu C, Cui G, Qu L, Bao M, Wang J, Chan Z, Wang Y (2020b) Integrating physiological and metabolites analysis

to identify ethylene involvement in petal senescence in Tulipa gesneriana. Plant Physiol Biochem 149: 121–131

Wang Z, Rong D, Chen D, Xiao Y, Liu R, Wu S, Yamamuro C (2021b) Salicylic acid promotes quiescent center cell division through ROS accumulation and down-regulation of PLT1, PLT2, and WOX5. J Integ Plant Biol 63: 583–596

Woo HR, Kim HJ, Nam HG, Lim PO (2013) Plant leaf senescence and death - regulation by multiple layers of control and implications for aging in general. J Cell Sci 126: 4823–4833

Woo HR, Kim HJ, Lim PO, Nam HG (2019) Leaf senescence: systems and dynamics aspects. Annu Rev Plant Biol 70: 347–376

Wu A, Allu AD, Garapati P, et al. (2012) JUNGBRUNNEN1, a reactive oxygen species-responsive NAC transcription factor, regulates longevity in Arabidopsis. Plant Cell 24: 482–506

Wu L, Ma N, Jia Y, Zhang Y, Feng M, Jiang CZ, Ma C, Gao J (2017) An ethylene-induced regulatory module delays flower senescence by regulating cytokinin content. Plant Physiol 173: 853–862

Wu X, Jiang L, Yu M, An X, Ma R, Yu Z (2016) Proteomic analysis of changes in mitochondrial protein expression during peach fruit ripening and senescence. J Proteom 147: 197–211

Yang SD, Seo PJ, Yoon HK, Park CM (2011) The Arabidopsis NAC transcription factor VNI2 integrates abscisic acid signals into leaf senescence via the COR/RD genes. Plant Cell 23: 2155–2168

Yang Z, Wang C, Qiu K, Chen H, Li Z, Li X, Song J, Wang X, Gao J, Kuai B, et al. (2020) The transcription factor ZmNAC126 accelerates leaf senescence downstream of the ethylene signalling pathway in maize. Plant Cell Environ 43: 2287–2300

Yu G, Xie Z, Lei S, Li H, Xu B, Huang B (2022) The NAC factor LpNAL delays leaf senescence by repressing two chlorophyll catabolic genes in perennial ryegrass. Plant Physiol http://dx.doi.org/10.1093/plphys/kiac070

Zhang K, Gan S (2012) An abscisic acid-AtNAP transcription factor-SAG113 protein phosphatase 2C regulatory chain for controlling dehydration in senescing Arabidopsis leaves. Plant Physiol 158: 961–969

Zhang K, Halitschke R, Yin C, Liu CJ, Gan SS (2013) Salicylic acid 3-hydroxylase regulates Arabidopsis leaf longevity by mediating salicylic acid catabolism. Proc Natl Acad Sci USA 110: 14807–14812

Zhang YM, Guo P, Xia X, Guo H, Li Z (2021) Multiple Layers of Regulation on Leaf Senescence: New Advances and Perspectives. Front Plant Sci 12: 788996

Zhao Y, Chan Z, Gao J, Xing L, Cao M, Yu C, Hu Y, You J, Shi H, Zhu Y, et al. (2016) ABA receptor PYL9 promotes drought resistance and leaf senescence. Proc Natl Acad Sci USA 113: 1949–1954

Zheng XY, Zhou M, Yoo H, Pruneda-Paz JL, Spivey NW, Kay SA, Dong X (2015) Spatial and temporal regulation of biosynthesis of the plant immune signal salicylic acid. Proc Natl Acad Sci USA 112: 9166–9173

Zou J, Lü P, Jiang L, Liu K, Zhang T, Chen J, Yao Y, Cui Y, Gao J, Zhang C (2021) Regulation of rose petal dehydration tolerance and senescence by RhNAP transcription factor via the modulation of cytokinin catabolism. Mol Hortic 1: 1–15